



ADDIS ABABA UNIVERSITY  
SCHOOL OF GRADUATE STUDIES  
ADDIS ABABA INSTITUTE OF TECHNOLOGY  
SCHOOL OF ELECTRICAL AND COMPUTER  
ENGINEERING

**Antenna Spacing Effects on Indoor  
MU-MIMO Channel Capacity**

By

**Feyissa Endebu**

**Advisor:**

**Dr. Murad Ridwan**

A Thesis submitted to Addis Ababa University in partial fulfillment of the requirements for the degree of Masters of science in Communication Engineering

April, 2016



# Dedication

Dedicated to my son Egnuma and his mom...

# Declaration

I, the undersigned, declare that this thesis work is my original work, has not been presented for a degree in this or any other universities, and all sources of materials used for the thesis work have been fully acknowledged.

Feyissa Endebu

Name

---

Signature

Place: Addis Ababa

---

Date of submission

This thesis has been submitted for examination with my approval as a university advisor.

Dr. Murad Ridwan

Advisor

---

Signature

# Abstract

In theory, multi-user MIMO is more immune to most of propagation limitations plaguing single-user MIMO (SU-MIMO) systems, such as channel rank loss or antenna correlation. However, in this thesis work, it has been considered the effect of antenna spacing on indoor multi-user MIMO sum-rate channel capacity at BS (base station) and user separation at UE (user equipment) side.

This can be analyzed by using correlation based-analytical approximation method, and its simulation results. These simulation results were obtained using MATLAB simulation tools. The simulation result shows the comparison of correlated MU-MIMO sum-rate channel capacity for all scenarios considered with non-correlated stochastic channel capacity.

Based on the result obtained it is better to use antenna spacing above  $\frac{1}{2}\lambda$  (half-carrier wave length) to get optimum correlated sum-rate channel capacity in indoor LOS compared to uncorrelated iid gaussian non-fading channel. In non-line of site(NLOS) MU-MIMO BC, antenna spacing from  $\frac{1}{5}\lambda$  to  $\frac{1}{2}\lambda$  is enough to get better sum-rate channel capacity than other correlated channel compared to uncorrelated Rayleigh fading channel capacity. Similarly, using Ricean fading channels, it is better to use antenna spacing above  $\frac{1}{2}\lambda$  to get optimum sum-rate channel capacity.

**KEY WORDS:** *MU-MIMO, Indoor Scenario, Antenna Spacing, User separation, Sum-Rate Channel Capacity*

# Acknowledgment

Foremost, I would like to thank my advisor, Dr.Murad Ridwan, for his guidance, patience and full support during the past one year. I am grateful to him for his encouragement and patience, especially during the time I needed these most. I am constantly surprised by his technical intuition, and I hope I have learned a bit from him in the way of thinking and carrying out thesis work.

My life here has been an enjoyable journey due to all my friends, brother and all the kind people I have met, at AAiT or outside AAiT. Their characters have enriched my own. In particular, I want to thank Tesfaye Mola and Gadissa Endebu for their endless support in material and financial.

Last, but not the least, I want to thank all my family members in Debra Berhan and Ambo for their support.

# Contents

<b>Declaration</b>	<b>ii</b>
<b>Abstract</b>	<b>iii</b>
<b>Acknowledgment</b>	<b>iv</b>
<b>List of Figures</b>	<b>vii</b>
<b>List of Tables</b>	<b>ix</b>
<b>1 Introduction</b>	<b>1</b>
1.1 Motivation . . . . .	1
1.1.1 Multiuser Multiple-Input Multiple-Output (MU-MIMO) . . . . .	2
1.1.2 Multiuser Multiple-Input Multiple-Output (MU-MIMO) basics . . . . .	3
1.1.3 Multi-User MIMO (MU-MIMO) Advantages . . . . .	4
1.1.4 Challenges of Multi-User MIMO (MU-MIMO) . . . . .	5
1.2 The Research Statements of Problem . . . . .	6
1.3 Literature Review and Related Works . . . . .	7
1.4 Objectives . . . . .	9
1.4.1 General Objectives . . . . .	9
1.4.2 Specific Objectives . . . . .	9
1.5 Research Methodologies . . . . .	10
1.6 Thesis Outlines . . . . .	10
<b>2 MIMO Wireless Communication</b>	<b>11</b>
2.1 Introduction . . . . .	11
2.2 MIMO Transmission Schemes . . . . .	12
2.2.1 Single Input Single Output (SISO) . . . . .	12
2.2.2 Single Input Multiple Output (SIMO) . . . . .	13
2.2.3 Multiple Input Single Output (MISO) . . . . .	13
2.2.4 Multiple Input Multiple Output (MIMO) . . . . .	14
2.3 MIMO Channel Capacity . . . . .	17

2.3.1	Capacity of Deterministic MIMO Channel . . . . .	17
2.3.2	Capacity of Non-Deterministic or Random MIMO Channels . . . . .	18
2.4	MIMO Channel Models . . . . .	19
2.4.1	MIMO Channel Model Classification . . . . .	19
2.5	Statistical Properties of the Channel Matrix . . . . .	22
2.5.1	Degrees of Freedom and Diversity . . . . .	22
2.5.2	Dependency on Antenna Spacing . . . . .	23
2.5.3	iid Rayleigh Fading Model . . . . .	23
2.5.4	Spatial Correlation . . . . .	24
2.5.5	Singular Values and Eigenvalues . . . . .	26
2.6	Analytical Models . . . . .	27
2.6.1	Correlation-Based Analytical Models . . . . .	27
<b>3</b>	<b>Multi-User MIMO Communication</b>	<b>31</b>
3.1	Introductions . . . . .	31
3.2	Channel State Information . . . . .	33
3.2.1	Instantaneous CSI . . . . .	33
3.2.2	Statistical CSI . . . . .	34
3.3	Antenna Spacing and Correlations . . . . .	35
3.3.1	Antenna Radiation Pattern . . . . .	35
3.3.2	Antenna Lobe . . . . .	36
3.3.3	Grating Lobes in Antenna Arrays . . . . .	37
3.4	Uplink-Multiple Access Multiuser-MIMO . . . . .	38
3.5	Downlink-Broadcasting Multiuser-MIMO . . . . .	40
3.6	Indoor Scenario Consideration . . . . .	41
<b>4</b>	<b>Simulation Result and Discussion</b>	<b>43</b>
4.1	Introduction . . . . .	43
4.2	Flow Chart . . . . .	45
4.3	Antenna Spatial Correlation . . . . .	45
4.4	Channel Capacity . . . . .	46
4.5	Simulation Results and Discussion . . . . .	46
4.5.1	Antenna Radiation Pattern . . . . .	46
4.6	Spatial correlations . . . . .	48
<b>5</b>	<b>Conclusion and Recommendation</b>	<b>59</b>
5.1	Conclusion . . . . .	59
5.2	Drawbacks . . . . .	60
5.3	Recommendation for Future Works . . . . .	60



**Bibliography**

**62**

**Appendix**

**65**

# List of Figures

1.1	MU-MIMO block diagram [3]	2
1.2	Block diagram of multi-user MIMO up link system [5]	3
1.3	Block diagram of multi-user MIMO down link system [5]	4
2.1	SISO model	12
2.2	SIMO model	13
2.3	MISO model	14
2.4	MIMO model	15
2.5	MIMO channel capacity with increasing number of antennas [15]	16
2.6	Classification of MIMO channel and propagation models[13]	20
2.7	Geometry of a MIMO channel with transmits and receives linear antenna arrays [13]	27
3.1	Antenna Pattern Parameters [27]	37
3.2	MIMO-MAC with single antenna users	38
3.3	MIMO-BC with M antenna base stations	40
4.1	Simulation flow chart	45
4.2	Antenna radiation pattern for different spacing	47
4.3	Effects of antenna spacing on spatial correlation at BS	48
4.4	Effects of user separation in LOS on spatial correlation	49
4.5	Effects of user separation in NLOS on spatial correlation	49
4.6	(4xTX, 4xRX) MIMO-BC Sum-rate channel capacity which shows the effect of antenna spacing below $0.5\lambda$ as compared to iid Rayleigh fading channel capacity in indoor NLOS.	50
4.7	(4xTX, 4xRX) MIMO-BC Sum-rate channel capacity which shows the effect of antenna spacing above $0.5\lambda$ as compared to iid Rayleigh fading channel capacity in indoor NLOS.	51
4.8	(4xTX, 4xRX) MIMO-BC Sum-rate channel capacity which shows the effect of antenna spacing above $0.5\lambda$ as compared to Gaussian iid channel capacity in indoor LOS.	52

4.9	(4xTX, 4xRX) MIMO-BC Sum-rate channel capacity which shows the effect of antenna spacing below $0.5\lambda$ as compared to Gaussian iid channel capacity in indoor LOS. . . . .	53
4.10	(4xTX, 4xRX) MIMO-MAC Sum-rate channel capacity which shows the effect average separation distance of sparsely randomly distributed users in 25m coverage areas in and indoor NLOS. . . . .	54
4.11	(4xTX, 4xRX) MIMO-MAC Sum-rate channel capacity which shows the effect average separation distance of randomly distributed users in 10m coverage areas in an indoor LOS. . . . .	55
4.12	(4xTX, 8xRX) MIMO-BC Sum-rate channel capacity which shows the effects antenna spacing below and above $0.5\lambda$ in indoor scenarios. . . . .	56
4.13	(4xTX, 8xRX) MIMO-BC Sum-rate channel capacity which shows the effects antenna spacing below and above $0.5\lambda$ in indoor scenarios. . . . .	57
4.14	(8xTX, 4xRX) MIMO-MAC Sum-rate channel capacity which shows the effects random user separation in indoor scenarios . . . . .	58

# List of Tables

3.1	Indoor correlation matrix . . . . .	42
4.1	Simulation parameters . . . . .	44

# List of Abbreviation and Acronyms

<b>AP</b>	Access Point
<b>AoA</b>	Angle of Arrival
<b>AoD</b>	Angle of Departure
<b>AWGN</b>	Additive White Gaussian Noise
<b>BC</b>	Broadcasting Channel
<b>BS</b>	Base Station
<b>CDMA</b>	Code Division Multiple Access
<b>CSI</b>	Channel State Information
<b>DAS</b>	Distributed Antenna System
<b>DPC</b>	Dirty Paper Coding
<b>DSP</b>	Digital Signal Processing
<b>EVD</b>	Eigen Value Decomposition
<b>FDMA</b>	Frequency Division Multiple Access
<b>FNBW</b>	First-Null Beam Width
<b>GSCM</b>	Geometry-based Stochastic Channel Models
<b>HPBW</b>	Half-Power Beam Width
<b>IEEE</b>	Institute of Electrical and Electronics Engineers
<b>iid</b>	independent and identically distributed
<b>LOS</b>	Line-Of-Sight

<b>MAC</b>	Multiple Access Channel
<b>MEA</b>	Multiple Element Antenna
<b>MIMO</b>	Multiple-Input Multiple-Output
<b>MISO</b>	Multiple Input Single Output
<b>MMSE</b>	Minimum Mean Square Error
<b>MU</b>	Mobile Unit
<b>MU-MIMO</b>	Multi-User Multiple-Input Multiple-Output
<b>NLOS</b>	Non-Line-Of-Sight
<b>PAS</b>	Power Azimuth Spectrum
<b>QRD</b>	Queer Resource Decomposition
<b>RRU</b>	Radio Resource Unit
<b>SDMA</b>	Space Division Multiple Access
<b>SIMO</b>	Single Input Multiple Output
<b>SISO</b>	Single Input Single Output
<b>SNR</b>	Signal to Noise Ratio
<b>SU-MIMO</b>	Single-User Multiple-Input Multiple-Output
<b>SVD</b>	Singular Value Decomposition
<b>TDMA</b>	Time Division Multiple Access
<b>UE</b>	User Equipment
<b>WLAN</b>	Wireless Local Area Network
<b>3GPP</b>	Third Generation Group Partnership
$\otimes$	Kronecker-Product
$\Lambda$	Diagonal of eigenvalue
$\lambda$	Carrier wavelength
$\rho$	Correlation coefficient

$\phi$	Angle of incidence
$\odot$	Schur-Hadamard product
$\Omega$	Coupling matrix
$A$	Angular power spectrum
$\Delta$	Angular spread
$\Sigma$	Diagonal singular value

# Chapter 1

## Introduction

### 1.1 Motivation

Wireless communication systems have become more and more important as they provide a flexibility and user friendly of application. Because of broadband wireless systems benefit, from accurate channel characterization there is growing interest in broadband wireless multiple-input multiple-output channel models and channel characterizations [1]. Most of the broadband traffic in today's world can be accounted from indoor environments. For supporting such high rate applications in indoor environments, and to provide a future proof infrastructure installation, optical fibers are becoming very popular.

Wireless coverage, on the other hand, offers the users with the much needed freedom of mobility. It is expected that by 2016, [29] more than 70 percent of the data traffic will be video traffic, but more important, it is estimated that 85 percent of the total traffic will come from indoors locations, with others raising this number up to 95 percent [29]. The indoor propagation scenario contains Line-Of-Sight (LOS) and more of Non-Line Of-Sight.

Multiple-Input-Multiple-Output (MIMO) systems offer significant increase data throughput without additional bandwidth or transmit power. It uses multiple antennas at transmitter and receiver front end. Since the use of antenna arrays in wireless communication systems provides many advantages. For example channel capacity can be greatly increased with increasing antenna array at both links [1, 2].



### 1.1.1 Multiuser Multiple-Input Multiple-Output (MU-MIMO)

Multi-user multiple-input multiple-output (MU-MIMO) systems are the wireless industry's current frontier towards satisfying the increasing demand of wireless high speed services. The optimal signal processing technique in the down-link of MU-MIMO system is dirty-paper coding (DPC). Unfortunately, DPC is far too complex for practical implementation, and merely serves as the theoretical benchmark [2].

Most practical signal processing techniques that have been proposed are linear, except for popular vector-perturbation based schemes. In general, a linear processing result in capacity losses (in Shannon sense) compared to DPC, but is still preferred due to complexity reasons [1, 2, 3]. In Figure 1:1, the base station (BS) transmit different signal through  $H_1$ ,  $H_2$  and  $H_3$  channels to  $MS_1$ ,  $MS_2$  and  $MS_3$  mobile users. However, this thesis work it was considered the effects antenna spacing on indoor MU-MIMO channel capacity typically encountered in building at BS (base station) antennas and user separation at the UE (user equipment) side.

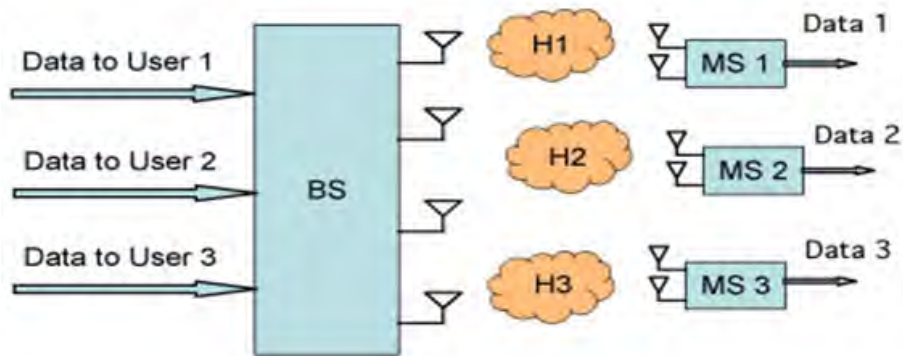


Figure 1.1: MU-MIMO block diagram [3]

In a multiuser MIMO (MU-MIMO) system, a base station communicates with multiple users. On the down-link known as the MIMO broadcast channel, the base station sends different information streams to the users. On the up-link, the base station receives different information from the users. Other variations of MU-MIMO involve full or partial multi-cast of data. Note that while MU-MIMO is often discussed in the context of cellular communication, it could conceivably be used in wireless local area networks or in wireless ad-hoc networks[3].

### 1.1.2 Multiuser Multiple-Input Multiple-Output (MU-MIMO) basics

The Multi-User-Multiple-Input-Multiple-Output (MU-MIMO) provides a methodology whereby spatial sharing of channels can be achieved. This can be achieved at the cost of additional hardware filters and antennas. But the incorporation does not come at the expense of additional bandwidth as is the case when technologies such as FDMA, TDMA or CDMA are used. When using spatial multiplexing in MU-MIMO the interference between the different users on the same channel is accommodated by the use of additional antennas, and additional processing when enables the spatial separation of the different users [1, 3]. There are two scenarios associated with Multi-user MIMO (MU-MIMO) [3, 4]:

1. Uplink - Multiple Access Channel (MAC) MU-MIMO: The development of the MU- MIMO- MAC is based on the known single user MIMO concepts broadened out to account for multiple users [2, 3]. The BS will coherently detect the signals transmitted as  $x_1, x_2, \dots, x_k$  from  $K$  users. Then the base station receive data as  $D_1, D_2, D_3, \dots, D_K$  and the received signal vector  $y_1, y_2, \dots, y_k$  together with knowledge of the CSI. When  $Q_1, Q_2, \dots, Q_k$  are the transmitted signal covariance. Since  $M_{T1}, M_{T2}, \dots, M_{TK}$  and  $1, 2, 3, \dots, M_R$  are the transmitter and receiver antenna elements. The channel estimate can be obtained from up link training [4].

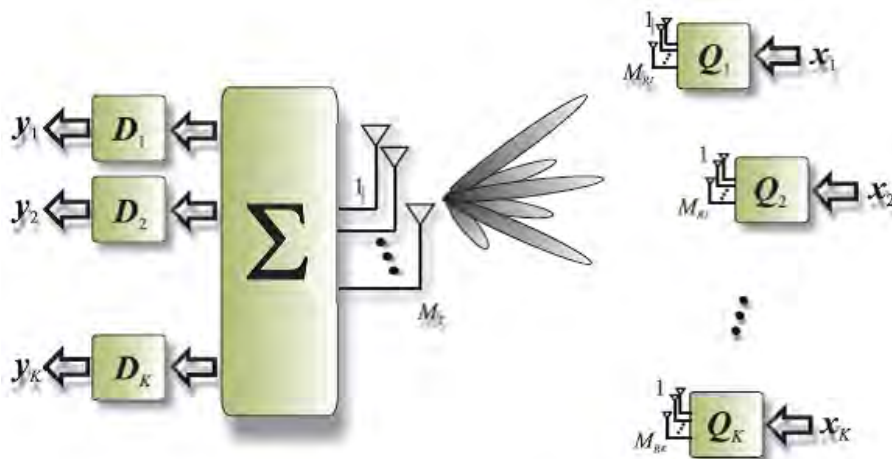


Figure 1.2: Block diagram of multi-user MIMO up link system [5]

2. The MIMO-BC is the more challenging scenario: The optimum strategy involves pre-interference cancellation techniques known as Dirty Paper Coding (DPC) [2, 3]. The MU-MIMO on the down link is especially interesting because the MIMO sum capacity can scale with the minimum of the number of

base station antennas and the sum of the number of users times the number of antennas per user. Where  $x_1, x_2, x_3, \dots, x_k$  and  $F_1, F_2, F_3, \dots, F_k$  are the transmitter signal vector and symbols. And where,  $G_1, G_2, G_3, \dots, G_k$  and  $y_1, y_2, y_3, \dots, y_k$  are receiver devices and received signal vectors.

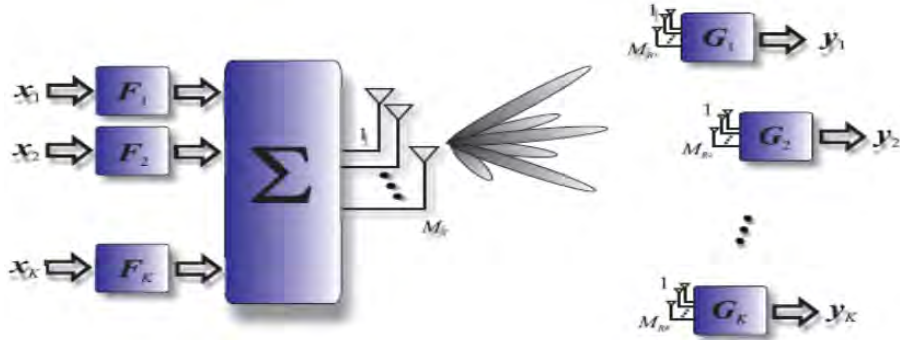


Figure 1.3: Block diagram of multi-user MIMO down link system [5]

This means that MU-MIMO can achieve MIMO capacity gains with a multiple antenna base station and a bunch of single antenna mobile users. This is of particular interest since real estate for multiple antennas is limited on small hand held devices [4].

### 1.1.3 Multi-User MIMO (MU-MIMO) Advantages

Multi-user MIMO (MU-MIMO) offers some significant advantages over other techniques [4, 5]. These are:

- MU-MIMO systems enable a level of direct gain to be obtained in a multiple access capacity arising from the multi-user multiplexing schemes. This is proportional to the number of base station antennas employed.
- MU-MIMO appears to be affected less by some propagation issues that affect single user MIMO systems. These include channel rank loss and antenna correlation although channel correlation still affects diversity on a per user basis; it is not a major issue for multi-user diversity.
- MU-MIMO allows spatial multiplexing gain to be achieved at the base station without the need for multiple antennas at the UE. This allows for the production of cheap remote terminals the intelligence and cost is included within the base station.

### 1.1.4 Challenges of Multi-User MIMO (MU-MIMO)

- Channel state information: in order to achieve high spatial multiplexing gain, the BS needs to process the received signals coherently. This requires accurate and timely acquisition of CSI. This can be challenging, especially in high mobility scenarios [4].
- There exists multiuser interference, hence complicated interference reduction or cancellation techniques should be used. For example, maximum likelihood multiuser detection for up-link dirty paper coding (DPC) techniques for down link, and interference alignment [4].
- Since several users are served on the same time-frequency resource, scheduling schemes which optimally select the group of users depending on the pre-coding detection schemes, CSI knowledge etc., should be considered. This increases the cost of the system implementation [4].
- Pilot contamination: in practical cellular networks, due to the limitation of the channel coherence interval, non-orthogonal pilot sequences have to be utilized in different cells. Therefore, the channel estimate obtained in a given cell is contaminated by pilots transmitted by users in other cells. This effect, called pilot contamination, reduces the system performance [4].

## 1.2 The Research Statements of Problem

Wireless channel has an application over a wide area but its performance differs from environment to environment (i.e. indoor and outdoor) because wireless channels feature fading, shadowing, interference, and other impairments that make the channel unpredictable. In today's wireless networks, there is an increasing demand for service quality, high data rates, network coverage, and lesser processing time. The scarcity of two fundamental resources for communications, namely, energy and bandwidth, is a serious challenge to fulfill these demands.

Nowadays, [29] indoor wireless network users are the predominant and it is estimated that by 2016, 85 percent of the total traffic will come from indoors locations in any kind of data traffic. MU-MIMO has the potential to combine the high throughput achievable with MIMO processing with the benefits of space division multiple accesses (SDMA). And, in an indoor scenario there are possibilities of transmitting base station and multiple users to be in the same building, on the same floor and may be in the same offices; which are the headache for mobile network operator to keep the user orthogonality in space.

Here in this thesis, a strong attention is given on the problem arrived because of spatial correlation. Spatial correlation affects the performance of wireless network by having an effect on the channel capacities. As a result here, to overcome the problem, the optimization of antenna spacing at BS and user separation on UE side is studied as an alternative means of alleviating the problem arrived because of spatial correlation.

### 1.3 Literature Review and Related Works

Multi User MIMO is advanced MIMO system used for spectral efficiencies and throughput optimizations. Since, multiple antennas exist at the base station and at the UE side, it has been expected that multiple users are using single base station or multiple base stations with multiple antenna arrays spatial multiplexing. In indoor scenarios, it is known that the receiver and the transmitter can be in the same building, on the same floor may be in the same offices. For this reason, in indoor scenarios the most interesting thing is to mitigate interference due to spatial correlation by keeping sufficient antenna spacing in indoor MU-MIMO to enhance the sum-rate channel capacity.

The following related literatures revealed some interesting technologies and methods of mitigating interference at both transmitter and receiver sides of MU-MIMO and indoor MU-MIMO system.

Fredrik et al. investigated indoor MU-MIMO systems in narrow corridor environments, typically encountered in office buildings, universities, hospitals, etc. Started by performing a theoretical investigation of downlink signal processing techniques in order to establish what channel parameters influence the performance. Then, analyzed extensively channel measurements in order to obtain an understanding of the behavior of the predominant parameter [6].

Robert W. Heath Jr. et al. investigated that multiuser MIMO is an effective strategy for DAS even in the presence of out-of cell interference. It considered a narrow band DAS channel model with independent Gaussian distributed small-scale fading and distance-dependent path-loss. It compares centralized multiuser MIMO zero-forcing beam-forming with distributed multiuser MIMO zero-forcing beam-forming across all RRUs in a cell, in terms of area spectral efficiency [7].

Kyung et al. studied the transmit antenna selection in multi-user MIMO systems with pre-coding. The optimum and reduced complexity sub-optimum antenna selection algorithms are introduced. QR-decomposition (QRD) based antenna selection is investigated and the reason behind its sub-optimality is analytically derived. It introduces the conventional QRD-based algorithm and propose an efficient QRD-based transmit antenna scheme that is both implementation and performance efficient [8].

Pohl et al. examined the relation between antenna spacing and capacity of MIMO channels for indoor environments using physical channel model which is a ray tracing program. In [9], it has been confirmed also by measurements that in rich

scattering environments an antenna spacing below  $0.5\lambda$  is to reach nearly the full capacity predicted for multiple-antenna arrays in ideal and uncorrelated Rayleigh fading channels.

Furthermore, this research gap has been identified when talking about the antenna spacing effect at BS and user separation on UE sides in an indoor MU-MIMO channel capacity by using correlation based analytical channel modeling which was not done as far as dealt with all these literature and related works.

## 1.4 Objectives

### 1.4.1 General Objectives

The main objective of this thesis work is to find the effects of antenna spacing at BS and user separation on UE sides on an indoor MU-MIMO channel capacities and its contribution for further capacity enhancement.

### 1.4.2 Specific Objectives

The specific objectives of this thesis can be summarized as follows:

- To evaluate the effect antenna spacing at BS and user separation on MU sides in an indoor LOS and NLOS on spatial correlations.
- To evaluate an indoor MU-MIMO channel capacity with varying antenna spacing at BS and users separation on MU sides in an indoor LOS and NLOS in both MIMO-BC and MIMO-MAC.
- To get the effects of antenna spacing at BS and user separation on MU sides on an indoor MU-MIMO channel capacity and finding sufficient spacing of antennas at BS.
- To reduce interference due to indoor propagation scenarios and indoor multi-users, this means to reduce the effect of spatial correlation in indoor environments.
- To compare an indoor MU-MIMO channel capacity with varying antenna spacing at BS and users separation on UE sides in an indoor LOS and NLOS in both MIMO-BC and MIMO-MAC with i.i.d Gaussian channel capacity and i.i.d Rayleigh fading channel capacity respectively.



## 1.5 Research Methodologies

In this thesis work, it has been evaluated the effects of antenna spacing at BS and user separation at mobile unit sides by correlation based-analytical channel modeling. And also obtained better antenna spacing for optimum sum-rate channel capacity in MU-MIMO BC and effects user separation on sum-rate channel capacity in MU-MIMO MAC. The methods used to achieve the desired objectives of this thesis were as follows. First, related literature about MU-MIMO channel capacity and correlation based-analytical channel modeling reviewed. Second, the spatial correlation and indoor MU-MIMO channel capacity was combined by analytical approach. Then, has been MATLAB simulation tool is used for the analysis of correlation based-analytical channel modeling.

## 1.6 Thesis Outlines

This thesis work contains different parts. These are, Introduction part which includes the technological overview of the topic, the literature review, the statement of problems, the objective and methodologies. Part two is about MIMO wireless communication which contains MIMO schemes, MIMO channel capacity and MIMO channel modeling. Part three is about Multiuser MIMO communication which includes channel state information, MU-MIMO broad casting, MU-MIMO multiple access control and indoor scenario considerations. Part four contains simulation results and discussion. And part five includes conclusion and recommendation for future works.

# Chapter 2

## MIMO Wireless Communication

### 2.1 Introduction

The increase in spectral efficiency offered by MIMO systems is based on the utilization of space (or antenna) diversity at both the transmitter and the receiver. Due to the utilization of space diversity, MIMO systems are also referred to as multiple-element antenna systems (MEA). With a MIMO system, the data stream from a single user is de-multiplexed into  $n_T$  separate sub-streams. The number  $n_T$  equals the number of transmit antennas. Each sub-stream is then encoded into channel symbols. It is common to impose the same data rate on all transmitters, but adaptive modulation rate can also be utilized on each of the sub-streams [12]. The signals are received by  $n_R$  receive antennas. With this transmission scheme, there is a linear increase in spectral efficiency compared to a logarithmic increase in more traditional systems utilizing receive diversity or no diversity[25].

The high spectral efficiencies attained by a MIMO system are enabled by the fact that in a rich scattering environment, the signals from each individual transmitter appear highly uncorrelated at each of the receive antennas. When the signals are conveyed through uncorrelated channels between the transmitter and receiver, the signals corresponding to each of the individual transmit antennas have attained different spatial signatures. The receiver can use these differences in spatial signature to simultaneously and at the same frequency separate the signals that originated from different transmit antennas[12, 25].

It has been well recognized that MIMO is a key technology to fully exploiting multi-path propagation in broadband wireless communication systems. Spatial multiplexing gain can be obtained via the potential de-correlation between the channel coefficients of MIMO radio channel[25].

However, the spatial multiplexing gain depends on the multi-path richness, since non-fading channel doesn't include de-correlation and neither MIMO capacity gain. Also, channel model with zero correlation would give too optimistic results, since in field the correlation is rarely zero. Hence, it is important to have realistic channel model in evaluating the real MIMO performance[25].

## 2.2 MIMO Transmission Schemes

Depending upon number of antennas used in transmission, MIMO transmission scheme is divided into SISO, SIMO, MISO, and MIMO for wireless communication system as shown bellow [14].

### 2.2.1 Single Input Single Output (SISO)

Single input single output (SISO) is less complex and easier to make for wireless communication system to transmit and receive signal. Assume input data stream is  $S$ , channel is  $h_{11}$  and output data stream be the  $Y$ . Antenna configuration and input output relation of SISO system is shown in Figure 2.1. The channel capacity is poor as compare to other technique but system design is not complex.

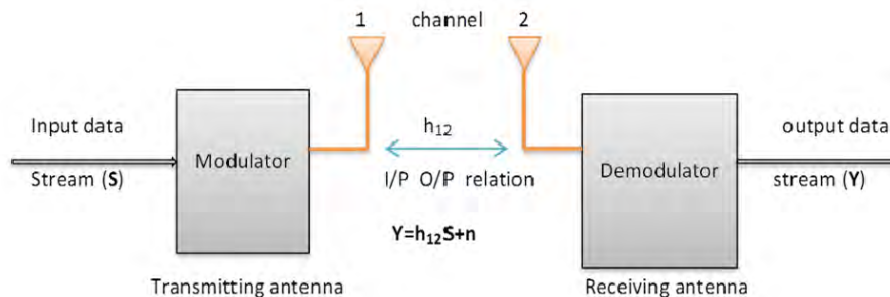


Figure 2.1: SISO model

$$C_{SISO} = B \log_2 \det(1 + SNR) \quad (2.1)$$

Where  $C$  is channel capacity,  $B$  is bandwidth of the signal,  $SNR$  is signal to noise ratio. SISO are advantageous in terms of the simplicity. It does not require processing in terms of diversity schemes. The throughput of the system depends upon the channel bandwidth and signal to noise ratio. In some conditions, these systems are exposed to the issues like multi-path effects[14].

### 2.2.2 Single Input Multiple Output (SIMO)

SIMO refers to the familiar wireless configuration with a single antenna at the transmitter and multiple antennas at receiver site. Now we assume we have two receiving signals  $Y_1$  and  $Y_2$  with different fading channel coefficient  $h_1$  and  $h_2$  with input data stream  $S$ . Antenna configuration and input output relation of SIMO (Receive Diversity) system is shown by Figure 2.2.

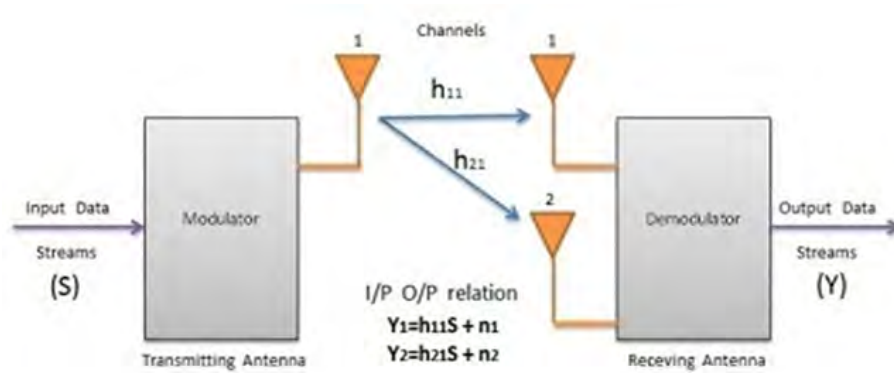


Figure 2.2: SIMO model

The channel capacity has not increased. The multiple receive antennas can help us get a stronger signal through diversity. The SIMO channel capacity is shown,

$$C_{SIMO} = M_r B \log_2 \det(1 + SNR) \quad (2.2)$$

where  $B$  is bandwidth, SNR is signal to noise ratio and  $M_r$  is the number of antennas used at the receiver side[14].

### 2.2.3 Multiple Input Single Output (MISO)

MISO system has multiple antennas at the transmitter and single antennas at receiver site. Now we assume we have two transmitting signals  $S_1$  and  $S_2$  with different fading channel coefficient  $h_1$  and  $h_2$  with output data stream  $Y$ . Antenna configuration and input output relation of MISO (transmit diversity) is given by Figure 2.3.

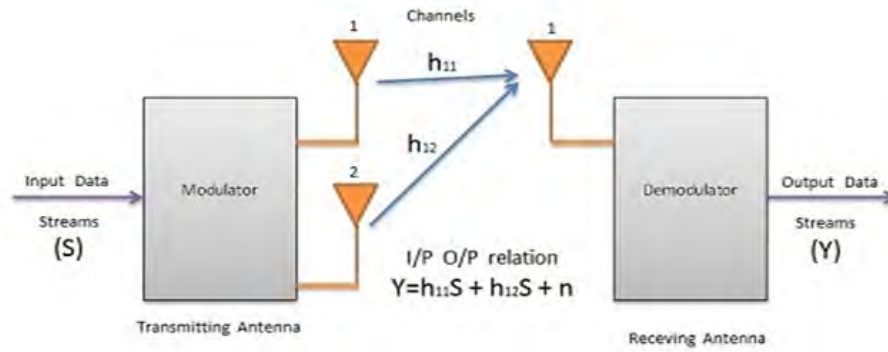


Figure 2.3: MISO model

The channel capacity has not really increased because we still have to transmit two signals at a time. The MISO capacity is,

$$C_{MISO} = M_t B \log_2 \det(1 + SNR) \quad (2.3)$$

where  $B$  is bandwidth, SNR is known as signal to noise ratio and  $M_T$  is the number of antennas used at the transmitter side[14].

## 2.2.4 Multiple Input Multiple Output (MIMO)

MIMO is a method of transmitting multiple data streams at the transmitter side and also receiving multiple data streams at the receiver side. MIMO antenna configuration describes that use of multiple transmit and multiple receive antennas for a single user produces higher capacity, spectral efficiency and more data rates for wireless communication. When the data rate is to be increased for a single user, this is called single user MIMO (SU-MIMO) and when the individual streams are assigned to various users; this is called multiuser MIMO (MU-MIMO) [14]. Antenna configuration and input output relation of MIMO (transmit diversity) is shown by Figure 2.4.

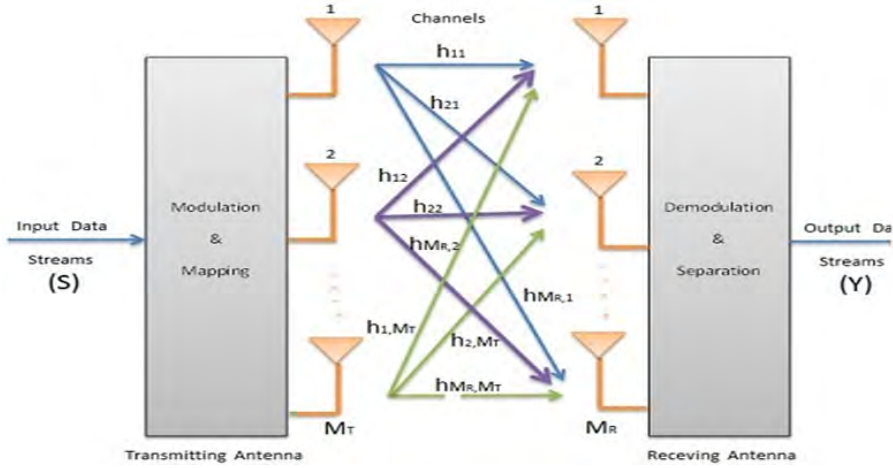


Figure 2.4: MIMO model

From the above Figure 2.4, output user data stream  $y = Hs + n$  (input output relation of MIMO channel), where  $S = [S_1, S_2, \dots, S_M]^T$  is the transmitted signal vector of order  $M_T \times 1$ ,  $y = [y_1, y_2, \dots, y_M]^T$  is the received signal vector of order  $M_R \times 1$ , and  $n = [n_1, n_2, \dots, n_M]^T$  is the Additive White Gaussian noise (AWGN) of order  $M_R \times 1$ . Let us consider a MIMO system with  $M_T$  transmit antennas and  $M_R$  receive antennas, denote the impulse response between the  $j^{th}$  ( $j = 1, 2, \dots, M_T$ ) transmit antenna and the  $i^{th}$  ( $i = 1, 2, \dots, M_R$ ) receiving antenna. Then MIMO channel can be represented using an  $M_R$  by  $M_T$  matrix format  $H$  is,

$$H = M_R \times M_T \quad (2.4)$$

where  $h_{ij}$  is a complex Gaussian random variable that models fading gain between the  $i^{th}$  transmit and  $j^{th}$  receive antenna. If a signal  $S_j(t)$  is transmitted from the  $j^{th}$  transmitted antenna, the signal receive at the  $i^{th}$  receive antenna. The input output relation is [14, 15],

$$y_i(t) = \sum_{j=1}^{M_t} h_{i,j} S_j(t), i = 1, 2, \dots, t, M_r \quad (2.5)$$

Here we take  $M_t$  transmit and  $M_r$  receive antennas with input data stream is  $S$  and output data stream is  $Y$ . MIMO has higher capacity as compare to other system. The MIMO capacity is given by,

$$C_{MIMO} = M_t M_r B \log_2(1 + SNR) \quad (2.6)$$

Where  $C$  is capacity,  $B$  is bandwidth, SNR is signal to noise ratio. Since  $M_t$  is the number of antennas used at the transmitter side and  $M_r$  is the number of antennas used at receiver side. Since the MIMO channel capacity increases with increasing number of transmit and receive antennas, it can be as shown in Figure 2.5 follow.

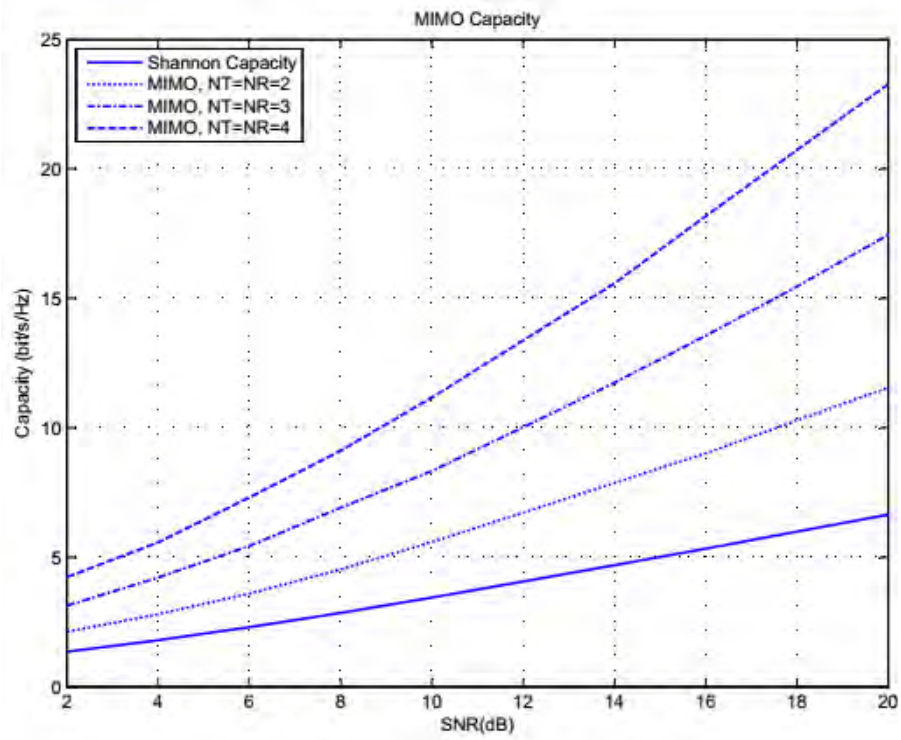


Figure 2.5: MIMO channel capacity with increasing number of antennas [15]

## 2.3 MIMO Channel Capacity

MIMO channel capacity can be evaluated for the following MIMO channel matrix cases:

1. Channel Matrix  $H$  is deterministic
2. Channel Matrix  $H$  is a random matrix

### 2.3.1 Capacity of Deterministic MIMO Channel

For a MIMO system of  $M_t$  transmit and  $M_r$  receive antennas received vector  $y$  can be written as

$$y = \sqrt{\frac{E_x}{M_t}} Hx + n \quad (2.7)$$

Where  $E_x$  is the energy of the transmitted signals and  $H$  is time-invariant channel matrix of  $M_r$  by  $M_t$  and  $n = [n_1, n_2, \dots, n_R]^T$  is a noise vector. Moreover, the autocorrelation of transmitted vector is defined as

$$R_{xx} = E[xx^H] \quad (2.8)$$

The autocorrelation of received matrix is defined as

$$\begin{aligned} R_{yy} &= E[yy^H] \\ &= E \left( \sqrt{\frac{E_x}{M_t}} Hx + n \right) \left( \sqrt{\frac{E_x}{M_t}} H^H x^H + n^H \right) \\ &= E \left( \frac{E_x}{M_t} Hxx^H H^H + nn^H \right) \\ &= \frac{E_x}{M_t} E(Hxx^H H^H) + E[nn^H] \\ &= \frac{E_x}{M_t} H E[xx^H] H^H + E[nn^H] \\ &= \frac{E_x}{M_t} H Q_x H^H + R_{nn} \end{aligned} \quad (2.9)$$

Where  $H^H$  is the complex conjugate transpose (Hermitian) of the matrix  $H$  in [14]. Now, the capacity of SISO channel can be easily be extended to MIMO capacity in  $bps/Hz$  when Channel State information (CSI) is not known at the transmitter which can be expressed as follows:

$$C = \log_2 \det \left( I_{M_R} + \frac{E_x}{M_T N_0} H H^H \right) \quad (2.10)$$



where  $\frac{E_x}{M_T} = \gamma$  is average Signal-to-Noise ratio of the receiving antenna and  $I_{M_R}$  is identity matrix. For no CSI at the transmitter the covariance matrix  $R_{xx}$  is identity matrix i.e.  $Q_x = I$ . Now, when the MIMO channel capacity when Channel State Information (CSI) is known at the transmitter in which case channel matrix  $H$  is a full rank matrix can be written as following

$$C = \left( \underset{\text{tr}(Q_x)=M_T}{\max} \right) \log_2 \det \left( I_{M_R} + \frac{\gamma}{M_T} H Q_x H^H \right) \quad (2.11)$$

### 2.3.2 Capacity of Non-Deterministic or Random MIMO Channels

The practical MIMO channels are essentially non-deterministic and time varying. Therefore, the channel matrix  $H$  is considered random and we assume random channel is ergodic process[13, 14]. MIMO channel capacity can be found by time average of the deterministic channel capacity in  $\text{bps}/\text{Hz}$  which can be given as follows:

$$C = E \left( \underset{\text{tr}(Q_x)=M_T}{\max} \right) \log_2 \det \left( I_{M_R} + \frac{\gamma}{M_T} H Q_x H^H \right) \quad (2.12)$$

This is considered as ergodic channel capacity of the MIMO channels. In general, MIMO channels are not independent and identically distributed (i.i.d). The channel correlation is closely related to the capacity of MIMO channels. Here we consider the capacity of MIMO channel when the channel gain between transmitter and receiver are correlated[13]. Now, we can consider the following correlated Kronecker channel model as

$$H = \sqrt{R_r} H_w \sqrt{R_t} \quad (2.13)$$

Where  $R_t$  is the correlation matrix and reflects the correlation between transmit antennas.  $R_r$  is the correlation matrix reflecting the correlation between receive antennas and  $H_w$  denoted the iid Rayleigh fading channel gain matrix. The diagonal entries of  $R_r$  and  $R_t$  are constrained to be unity. Then, substituting equation (2.14) into (2.10) we can write MIMO channel capacity as

$$C = \log_2 \det \left( I_{M_R} + \frac{\gamma}{M_T} \sqrt{R_r} H_w R_t H_w^H R_r^{\frac{H}{2}} \right) \quad (2.14)$$

Condition: If  $M_T = M = M_R$ ,  $R_t$  and  $R_r$  are full rank and SNR is high we can approximate above relation as

$$C \approx \log_2 \det \left( \frac{\gamma}{M_T} H_w H_w^H \right) + \log_2 \det(R_r) + \log_2 \det(R_t) \quad (2.15)$$

Equation (2.16) above shows that MIMO channel capacities have been reduced due to correlation between transmit and receive antennas by an amount equal to  $\log_2 \det(R_r) + \log_2 \det(R_t)$ . Increase in correlation usually causes a decrease in SNR[13, 14].

## 2.4 MIMO Channel Models

A set of spatial channel model parameters are specified that have been developed to characterize the particular features of MIMO radio channels. SISO channel models provide information on the distributions of signal power level and Doppler shifts of received signals. MIMO channel models, which are based on the classical understanding of multi-path fading and Doppler spread, incorporate additional concepts such as Angular Spread, Angle of Arrival, Power-Azimuth-Spectrum (PAS), and the antenna array correlation matrices for the transmitter ( $T_x$ ) and receiver ( $R_x$ ) combinations[13].

### 2.4.1 MIMO Channel Model Classification

A variety of MIMO channel models, many of them based on measurements. The proposed model can be classified in various ways. A potential way of distinguishing the individual model is with regard to type of channel that is being considered, i.e., narrow (flat fading) vs. broadband (frequency-selective) models, time-varying vs. time structure. In contrast, broadband (frequency-selectivity) channels require additional modeling of the multi-path channel characteristics. With time-varying channels, one additionally requires a model for the temporal channel evolution according to certain Doppler characteristics[13].

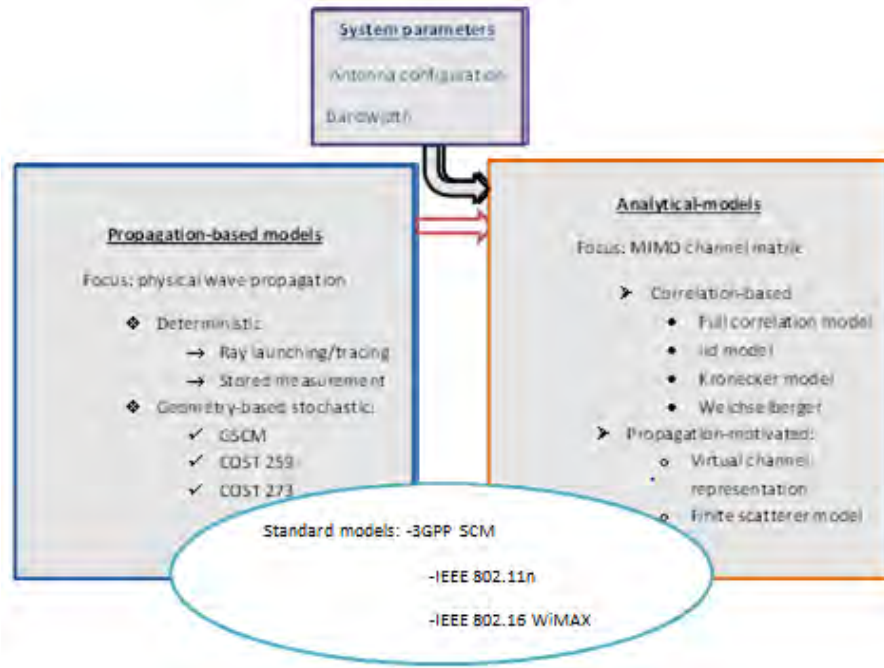


Figure 2.6: Classification of MIMO channel and propagation models[13]

The fundamental distinction is between physical channel models and correlation based-analytical channel model models. Physical channel models characterize an environment on the basis of electromagnetic wave propagation by describing the double directional multi-path propagation between the location of the transmit ( $T_x$ ) array and the location of the receive ( $R_x$ ) array. They explicitly model wave propagation parameters like the complex amplitude, AoD, AoA, and delay of MPC. More sophisticated models also incorporate polarization and time variation. Depending on the chosen complexity, physical model allow for an accurate reproduction of radio propagation[13].

Physical models are independent of antenna configurations (antenna pattern, number of antennas, array geometry, polarization, mutual coupling) and system bandwidth. Physical MIMO channel models can further be split into deterministic models, geometry-based stochastic models, and non-geometric stochastic models. Deterministic models characterize the physical propagation parameters in completely deterministic manner. With geometry-based stochastic channel models (GSCM), the impulse response is characterized by the laws of wave propagation applied to specific  $T_x$ ,  $R_x$  and scatterer geometries, which are chosen in a stochastic (random) manner. In contrast, non-geometric stochastic models describe and determine physical parameters (AoD, AoA, delay, etc.) in a completely stochastic way by prescribing underlying probability distribution functions without assuming an underlying geometry[13].

In contrast to physical models, analytical channel models characterize the impulse response (equivalently, the transfer function) of the channel between the individual transmit and receive antennas in a mathematical/analytical way without explicitly accounting for wave propagation. The individual impulse responses are subsumed in a (MIMO) channel matrix. Analytical models are very popular for synthesizing MIMO matrices in the context of system and algorithm development and verification. Analytical models can be further subdivided into propagation-motivated models and correlation-based models. The first subclass models the channel matrix via propagation parameters. Correlation-based models characterize the MIMO channel matrix statistically in terms of the correlations between the matrix entries. Popular correlation-based analytical channel models are the Kronecker model [7, 8, 9, 10] and the Weichselberger model [11].

For the purpose of comparing different MIMO systems and algorithms, various organizations defined reference MIMO channel models which establish reproducible channel conditions. With physical models this means to specify a channel model, reference environments, and parameter values for these environments. With analytical models, parameter sets representative for the target scenarios need to be prescribed. Examples for such reference models are the ones proposed within 3GPP, COST 259, COST 273, IEEE 802.16a, e, and IEEE 802.11n [7, 8, 9].

## 2.5 Statistical Properties of the Channel Matrix

### 2.5.1 Degrees of Freedom and Diversity

Given the statistical model, one can quantify the spatial multiplexing capability of a MIMO channel [13]. With probability 1, the rank of the random matrix  $H^a$  is given by

$$\text{rank}(H^a) = \min(N_r, N_c) \quad (2.16)$$

where  $N_r$  is number of non-zero rows and  $N_c$  is number of non-zero columns. This yields the number of degrees of freedom available in the MIMO channel. The number of non-zero rows and columns depends in turn on two separate factors:

- The amount of scattering and reflection in the multi-path environment. The more scatterers and reflectors there are, the larger the number of non-zero entries in the random matrix  $H^a$ , and the larger the number of degrees of freedom.
- The lengths  $L_t$  and  $L_r$  of the transmit and receive antenna arrays. With small antenna array lengths, many distinct multi-paths may all be lumped into single resolvable path. Increasing the array apertures allows the resolution of more paths, resulting in more non-zero entries of  $H^a$  and an increased number of degrees of freedom.

In a slow fading environment, another important parameter is the amount of diversity in the channel. This is the number of independent channel gains that have to be in a deep fade for the entire channel to be in deep fade. In the angular domain MIMO model, the amount of diversity is simply the number of non-zero entries in  $H_a$ .

Note that channels that have the same degrees of freedom can have very different amounts of diversity. The number of degrees of freedom depends primarily on the angular spreads of the scatters/reflectors at the transmitter and at the receiver, while the amount of diversity depends also on the degree of connectivity between the transmit and receive angles. In a channel with multiple-bounced paths, signals sent along one transmit angle can arrive at several receive angles. Such a channel would have more diversity than one with single-bounced paths with signal sent along one transmit angle received at a unique angle, even though the angular spreads may be the same [13].

## 2.5.2 Dependency on Antenna Spacing

Focusing on the case of critically spaced antennas (i.e., antenna separations  $\Delta t$  and  $\Delta r$  are half the carrier wavelength). Now the critical question is that; What is the impact of changing the antenna separation on the channel statistics? To answer this question, we vary the antenna separation at BS, or equivalently the number of antenna elements. Placing antennas more sparsely reduces the resolution of the antenna array and can reduce the number of degrees of freedom and the diversity of the channel. Placing the antennas more densely adds spurious basis vectors which do not correspond to any physical directions, and does not add resolvability. In terms of the angular channel matrix  $H^a$ , this has the effect of adding zero rows and columns; in terms of the spatial channel matrix  $H$ , this has the effect of making the entries more correlated [13].

Increasing the antenna separation within a given array length  $L$  does not increase the number of degrees of freedom in the channel. What about increasing the antenna separation while keeping the number of antenna elements  $n$  the same? This question makes sense if the system is hardware-limited rather than limited by the amount of space to put the antenna array in. Increasing the antenna separation this way reduces the beam width of the  $n$  angular basis beam forming patterns but also increases the number of main lobes in each. If the scattering environment is rich enough such that the received signal arrives from all directions, the number of non-zero rows of the channel matrix  $H^a$  is already  $n$ , the largest possible, and increasing the spacing does not increase the number of degrees of freedom in the channel [13].

On the other hand, if the scattering is clustered to within certain directions, increasing the separation makes it possible for the scattered signal to be received in more bins, thus increasing the number of degrees of freedom. In terms of the spatial channel matrix  $H$ , this has the effect of making the entries look more random and independent. At a base-station on a high tower with few local scatterers, the angular spread of the multi-paths is small and therefore one has to put the antennas many wavelengths apart to de-correlate the channel gains [13, 14].

## 2.5.3 iid Rayleigh Fading Model

A very common MIMO fading model is the i.i.d. Rayleigh fading model: the entries of the channel gain matrix  $H[m]$  are independent, identically distributed and circular symmetric complex Gaussian. Since the matrix  $H[m]$  and its angular

domain representation  $H^a[m]$  are related by

$$H^a[m] = U_r^* H[m] U_t \quad (2.17)$$

And  $U_r$  and  $U_t$  are fixed unitary matrices; this means that  $H_a$  should have the same i.i.d. Gaussian distribution as  $H$ . Thus, using the modelling approach described here, we can see clearly the physical basis of the i.i.d Rayleigh fading model, in terms of both the multipath environment and the antenna arrays. There should be a significant number of multi-paths in each of the resolvable angular bins, and the energy should be equally spread out across these bins. This is the so called richly scattered environment. If there are very few or no paths in some of the angular directions, then the entries in  $H$  will be correlated. Moreover, the antennas should be either critically or sparsely spaced. If the antennas are densely spaced, then some entries of  $H^a$  are approximately zero and the entries in  $H$  itself are highly correlated. However, by a simple transformation, the channel can be reduced to an equivalent channel with fewer antennas which are critically spaced [13, 14].

Compared to the critically spaced case; having sparser spacing makes it easier for the channel matrix to satisfy the i.i.d. Rayleigh assumption. This is because each bin now spans more distinct angular windows and thus contains more paths, from multiple transmit and receive directions. This substantiates the intuition that putting the antennas further apart makes the entries of  $H$  less dependent. On the other, if the physical environment already provides scattering in all directions, then having critical spacing of the antennas is enough to satisfy the i.i.d. Rayleigh assumption.

Due to the analytical tractability, we will use the i.i.d. Rayleigh fading model quite often to evaluate performance of MIMO communication schemes, but it is important to keep in mind the assumptions on both the physical environment and the antenna arrays for the model to be valid [13].

## 2.5.4 Spatial Correlation

The originality of MIMO techniques lies in the exploitation of the spatial or double-directional structure of the channel. This structure is also largely responsible for the performance of MIMO systems. Therefore, it does make sense to introduce a way to characterize the spatial properties of a multi-antenna channel, or more specifically, the space-only correlation of the channel. For a MIMO channel with a limited number of antennas, we can switch from the double-directional notation to

a matrix notation, and therefore define the spatial correlation matrix as

$$R = \varepsilon(\text{vec}(H^H)\text{vec}(H^H)^H) \quad (2.18)$$

This matrix is a  $n_t n_r \times n_t n_r$  positive semi-definite Hermitian matrix, which describes the correlation between all pairs of transmit-receive channels. Depending on which channel pairs are chosen, several correlations can be defined:

- If both channels share the same transmit and receive antennas  $m$  and  $n$ ,  $\varepsilon(H(n, m)H(n, m)^*)$  Simply represents the average energy of the channel between antenna  $m$  and antenna  $n$ .
- If both channels share the same transmit antenna,  $r_m^{(nq)} = \varepsilon(H(n, m)H(q, m)^*)$  represents the receive correlation between channels originating from transmit antenna  $m$  and impinging upon receive antennas  $n$  and  $q$ .
- If both channels share the same receive antenna,  $t_n^{(mp)} = \varepsilon(H(n, m)H(n, p)^*)$  represents the transmit correlation between channels originating from transmit antennas  $m$  and  $p$  and arriving at receive antenna  $n$ .
- If both channels originate from different transmit antennas, and arrive at different receive antennas,  $\varepsilon(H(n, m)H(q, p)^*)$  is simply defined as the cross-channel correlation between channels  $(m, n)$  and  $(q, p)$ .

The facts that all these covariance are correlations between channels, despite the fact that some are called transmit or receive antenna correlations for simplicity. It is also convenient to define transmit and receive correlation matrices  $R_t$  and  $R_r$  as

$$R_t = \varepsilon(H^H H) \quad (2.19)$$

$$R_r = \varepsilon(H H^H) \quad (2.20)$$

For homogeneous channels, the correlation coefficient between two individual channels is directly related to the joint angular power spectrum  $A(\Omega_t, \Omega_r)$ , while transmit and receive correlation is related to  $A_t(\Omega_t)$  respectively ( $A_r(\Omega_r)$ ). As an example, assuming 2-D propagation, the transmit correlation between two antennas can be written as

$$t = \int_0^{2\pi} e^{j\phi_t(\theta_t)} A_t(\theta_t) d\theta_t \quad (2.21)$$

where, for convenience, the transmit azimuth power spectrum with respect to the relative azimuth. Two extreme cases are worth mentioning here. The first case corresponds to a very rich scattering environment around the transmitter with a uniform distribution of the energy, so that  $A_t(\theta_t) \approx \frac{1}{2\pi}$ . The transmit correlation then reads



as

$$\begin{aligned}
t &= \frac{1}{2\pi} \int_0^{2\pi} e^{j\Phi_t(\theta_t)} A_t(\theta_t) d\theta_t \\
&= \frac{1}{2\pi} \int_0^{2\pi} e^{j2\pi(\frac{d_t}{\lambda})\cos(\theta_t)} d\theta_t \\
&= J_0\left(\frac{2\pi d_t}{\lambda}\right)
\end{aligned} \tag{2.22}$$

The transmit correlation only depends on the spacing between the two considered antennas. The second extreme case occurs when scatterers around the transmit array are concentrated along a narrow direction  $\theta_{(t,0)}$ , i.e. at  $(\theta_t) \rightarrow \delta(\theta_t - \theta_{(t,0)})$ . Such channel is also known as degenerate and causes a very high transmit correlation approaching one.

$$t = e^{j\Phi_t(\theta_{(t,0)})} = e^{j2\pi(\frac{d_t}{\lambda})\cos(\theta_{(t,0)})} \tag{2.23}$$

Interestingly, the scattering direction is directly related to the phase of the transmit correlation. Using the finite scatterer representation, and assuming that all paths are independent and have the same average power normalized to one, the antenna covariance are directly related to the steering vectors as

$$R_t = (A_t A_t^H)^T = A_t^* A_t^T \tag{2.24}$$

$$R_r = (A_r A_r^H)^T = A_r^* A_r^T \tag{2.25}$$

Where  $A_r$  and  $A_t$  represent the  $nr \times ns, r$  and  $nt \times ns, t$  matrices whose columns are the steering vectors related to the directions of each path observed at  $R_x$  and  $T_x$  (these matrices are in general not unitary). It is straight forward to prove that the first equation above is indeed equivalent to (2.19) in this case. Finally, it is interesting to consider the case when the energy spreading is very large at both sides and when the antenna inter-element spacing  $d_t$  and  $d_r$  are sufficiently large. In such scenarios, the various elements of  $H$  become uncorrelated, and  $R$  becomes diagonal[13, 14].

### 2.5.5 Singular Values and Eigenvalues

The channel matrix  $H$  is not always full rank. Denoting by  $r(H)$  the rank of  $H$ , the singular value decomposition (SVD) of the  $n_r \times n_t$  channel matrix reads as

$$H = U_H \Sigma_H V_H \tag{2.26}$$

Where  $U_H$  and  $V_H$  are  $n_r \times r(H)$  and  $n_t \times r(H)$  unitary matrices, and

$$\Sigma_H = \text{diag}(\sigma_1, \sigma_2, \dots, \sigma_{r(H)}) \tag{2.27}$$

is the diagonal matrix containing the ordered singular values of  $H$ . Denoting by  $n$  the minimum of  $n_t, n_r$ , the matrix  $W = HH^H$  (for  $n_t > n_r$ ) or  $W = H^H H$  (for  $n_t < n_r$ ) is an  $n \times n$  positive semi-definite Hermitian matrix, whose eigenvalue decomposition (EVD) is given by

$$W = U_w \Lambda_w U_w^H \quad (2.28)$$

Where  $\Lambda_w = \text{diag}(\lambda_1, \lambda_2, \dots, \lambda_n)$  contains the eigenvalues of  $W$  (i.e. the squared singular values of  $H$ ,  $r(H)$  of which are non-zero and equal to  $\lambda_1, \dots, \lambda_{r(H)} = (\sigma_1^2, \sigma_2^2, \dots, \sigma_{r(H)}^2)$ ). For notational convenience, we always write  $\lambda_k \equiv \lambda_k(W)$  [13].

## 2.6 Analytical Models

### 2.6.1 Correlation-Based Analytical Models

Various narrowband analytical models are based on a multivariate complex Gaussian distribution of the MIMO channel coefficients (i.e., Rayleigh or Ricean fading). The channel matrix can be split into a zero-mean stochastic part  $H_s$  and a purely deterministic part  $H_d$ . The Ricean MIMO channel  $H_{Ricean}$  can be modeled as the sum of a constant  $H_{LOS}$  and a variable Rayleigh component caused by scattering,

$$H_{Ricean} = \sqrt{\frac{K_r}{1 + K_r}} e^{j\Phi_0} H_{LOS} + \sqrt{\frac{1}{1 + K_r}} H_{Rayleigh} \quad (2.29)$$

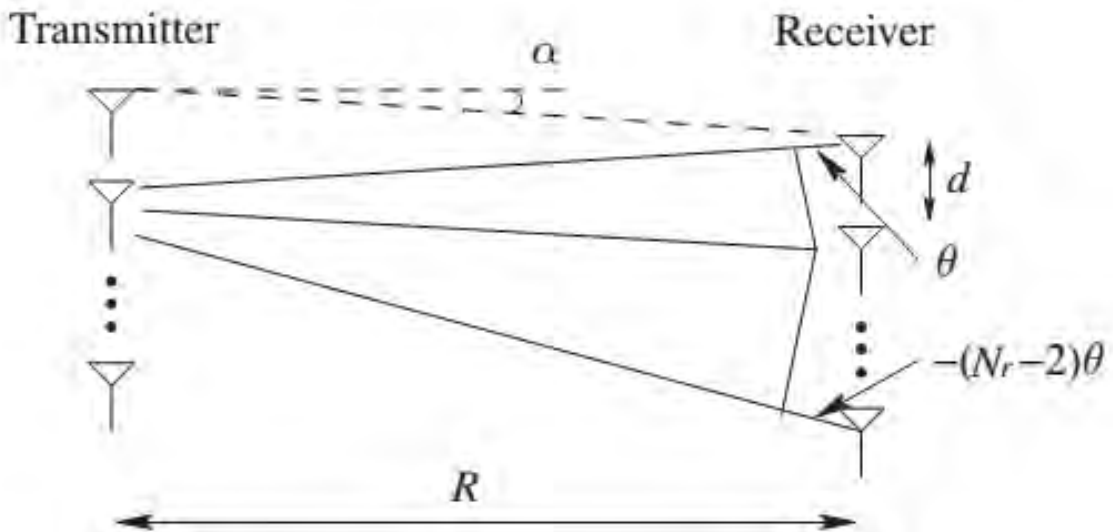


Figure 2.7: Geometry of a MIMO channel with transmits and receives linear antenna arrays [13]

Where  $K_r$  is the Ricean factor,  $\Phi_0$  is the phase shift of the signal due to

propagation from a transmit antenna element to a receive antenna element, and  $H_{Rayleigh} = H_w$ . Given a MIMO system with a uniform linear array of  $N_t$  transmit antennas and a uniform linear array of  $N_r$  receive antennas, as shown in Figure 2.7, when the distance  $R$  between the two arrays are very large, the  $H_{LOS}$  matrix can be derived as[13, 14].

$$H_{LOS} = d_r d_t^T = \begin{bmatrix} 1 & e^{j\theta} & \dots & e^{j(N_t-1)\theta} \\ e^{-j\theta} & 1 & \dots & e^{j(N_t-2)\theta} \\ \vdots & \vdots & \ddots & \vdots \\ e^{-j(N_r-1)\theta} & e^{-j(N_t-2)\theta} & \dots & 1 \end{bmatrix} \quad (2.30)$$

Where  $d_r$  and  $d_t$  are transmit and receive steering vectors, and  $\theta$  is the phase shift between two adjacent array elements. The second equality holds only when transmit and receive antennas are almost parallel. The existence of a Ricean component reduces the multipath richness. For a given SNR, the Ricean channel has a capacity lower than that of the Rayleigh fading channel, but is higher than that of the AWGN channel; it approximates the capacity of the Rayleigh fading channel as  $K_r \rightarrow 0$ , and that of the AWGN channel as  $K_r \rightarrow 1$ . However, for a given transmit power, the Ricean channel introduces a higher SNR, since there are no obstructions. For simplicity, we thus assume  $K_r = 0$  i.e.  $H_{Ricean} = H_{Rayleigh}$ . In its most general form, the zero-mean multivariate complex Gaussian distribution of  $h = \text{vec}H$  is given by

$$f(h) = \frac{1}{(\pi^{nk} \det R_H)} \exp(-h^H R_H^{-1} h) \quad (2.31)$$

The  $mk \times mk$  matrix  $R_H = E[hh^H]$  is known as full correlation matrix and describes the spatial MIMO channel statistics. It contains the correlations of all channel matrix elements. Realizations of MIMO channels with distribution (2.32) can be obtained by

$$H = \text{unvec}(h), h = R_H^{\frac{1}{2}} g \quad (2.32)$$

Here,  $R_H^{\frac{1}{2}}$  denotes an arbitrary matrix square root (i.e., any matrix satisfying  $R_H^{\frac{1}{2}} R_H^{\frac{H}{2}} = R_H$ ) and  $g$  is a  $mk \times 1$  vector with i.i.d. Gaussian elements with zero mean and unit variance. Note that direct use of (2.33) in general requires full specification of  $R_H$  which involves  $(mk)^2$  real-valued parameters. To reduce this large number of parameters, several different models were proposed that impose a particular structure on the MIMO correlation matrix. Some of these models will next be briefly reviewed[13].

## The iid Model

The simplest analytical MIMO model is the i.i.d. model (sometimes referred to as canonical model). Here  $R_H = \rho I$ , i.e., all elements of the MIMO channel matrix  $H$  are uncorrelated (and hence statistically independent) and have equal variance  $\rho$ . Physically, this corresponds to a spatially white MIMO channel which occurs only in rich scattering environments characterized by independent MPCs uniformly distributed in all directions. The i.i.d. model consists just of a single parameter (the channel power  $\rho$ ) and is often used for theoretical considerations like the information theoretic analysis of MIMO systems[8, 9, 10].

## The Kronecker Model

The so-called Kronecker model was used in [19, 20, 21] for capacity analysis before being proposed by [22] in the framework of the European Union SATURN project . It assumes that spatial  $T_x$  and  $R_x$  correlations are separable, which is equivalent to restricting to correlation matrices that can be written as Kronecker product

$$R_H = R_{T_x} \otimes R_{R_x} \quad (2.33)$$

with  $T_x$  and  $R_x$  correlation matrices  $R_{T_x} = E[H^H H]$ ,  $R_{R_x} = E[HH^H]$ , respectively. It can be shown that under the above assumption, (2.34) simplifies to the Kronecker model

$$h = \sqrt{(R_{T_x} \otimes R_{R_x})}g \rightarrow H = \sqrt{R_{R_x}}G\sqrt{R_{T_x}} \quad (2.34)$$

with  $G = \text{unvec}(g)$  an i.i.d. unit-variance MIMO channel matrix. The model requires specification of the  $T_x$  and  $R_x$  correlation matrices, which amounts to  $n^2 + m^2$  real parameters (instead of  $n^2 m^2$ ). The main restriction of the Kronecker model is that it enforces a separable AoD-AoA spectrum [20], i.e., the joint AoD-AoA spectrum is the product of the AoD spectrum and the AoA spectrum. Note that the Kronecker model is not able to reproduce the coupling of a single AoD with a single AoA, which is an elementary feature of MIMO channels with single-bounce scattering. Nonetheless, the model (2.34) has been successfully used for the theoretical analysis of MIMO systems and for MIMO channel simulation. Furthermore, it allows for independent array optimization at  $T_x$  and  $R_x$ . These applications and its simplicity have made the Kronecker model quite popular.

## The Weichselberger Model

The Weichselberger model [20, 22] aims at obviating the restriction of the Kronecker model to separable AoA-AoD spectra that neglects significant parts of the spatial structure of MIMO channels. Its definition is based on the eigenvalue decomposition of the  $T_x$  and  $R_x$  correlation matrices,  $R_{T_x} = U_{T_x}\Lambda_{T_x}U_{T_x}^H$ ,  $R_{R_x} = U_{R_x}\Lambda_{R_x}U_{R_x}^H$ . Here,  $U_{T_x}$  and  $U_{R_x}$  are unitary matrices whose columns are the eigenvectors of  $R_{T_x}$  and  $R_{R_x}$ , respectively, and  $\Lambda_{T_x}$  and  $\Lambda_{R_x}$  are diagonal matrices with the corresponding eigenvalues. The model itself is given by

$$H = U_{R_x}(\Omega \odot G)U_{T_x}^T \quad (2.35)$$

where  $G$  is again an  $n \times m$  i.i.d. MIMO matrix,  $\odot$  denotes the Schur-Hadamard product (element-wise multiplication), and  $\Omega$  is an  $n \times m$  coupling matrix whose (real-valued and non-negative) elements determine the average power coupling between the  $T_x$  and  $R_x$  eigenmodes. This coupling matrix allows for joint modeling of the  $T_x$  and  $R_x$  channel correlations. We note that the Kronecker model is a special case of the Weichselberger model obtained with the rank-one coupling matrix  $\Omega = \lambda_{R_x}\lambda_{T_x}$ , where  $\lambda_{T_x}$  and  $\lambda_{R_x}$  are vectors containing the eigenvalues of the  $T_x$  and  $R_x$  correlation matrix, respectively. The Weichselberger model requires specification of the  $T_x$  and  $R_x$  eigenmodes  $U_{T_x}$  and  $U_{R_x}$  and of the coupling matrix  $\Omega$ . In general, this amounts to  $n(n-1) + m(m-1) + nm$  real parameters [20, 22].

We emphasize, however, that capacity (mutual information) and diversity order of a MIMO channel are independent of the  $T_x$  and  $R_x$  eigenmodes; hence, their analysis requires only the coupling matrix  $\Omega$  ( $nm$  parameters). In particular, the structure of  $\Omega$  determines which MIMO gains (diversity, capacity, or beamforming gain) can be exploited.

# Chapter 3

## Multi-User MIMO Communication

### 3.1 Introductions

In this chapter, we focus to multiuser channels and study the role of multiple antennas in both the uplink (many-to-one) and the downlink (one-to-many). In addition to allowing spatial multiplexing and providing diversity to each user, multiple antennas allow the base-station to simultaneously transmit or receive data from multiple users. Again, this is a consequence of the increase in degrees of freedom from having multiple antennas [18]. Independent data streams are sent at the different transmit antennas, and no cooperation across transmit antennas is needed.

Equating the transmit antennas with users, these receiver structures can be directly used in the uplink where the users have a single transmit antenna each but the base-station has multiple receive antennas; [18] this is a common configuration in cellular wireless systems. It is less apparent how to come up with good strategies for the downlink, where the receive antennas are at the different users; thus the receiver structure has to be separate, one for each user. However, as will see, there is an interesting duality between the uplink and the downlink, and by exploiting this duality, one can map each receive architecture for the uplink to a corresponding transmit architecture for the downlink. In particular, there is an interesting precoding strategy, which is the transmit dual to the receiver-based successive cancellation strategy.

It has been shown that time division multiple access (TDMA) systems cannot achieve a linear increase of the sum-rate capacity of multi-user (MU) MIMO systems in the number of transmit antennas. The solution to this problem is to serve user's

simultaneously using space-division multiple access (SDMA). The information theoretic results in [13, 14, 15, 16] and [17] have shown that it is necessary to use some kind of Costa's "dirty-paper" coding (DPC) or Tomlinson-Harashima precoding to reach the sum capacity of a multi-user MIMO downlink system. DPCs achieve the maximum sum rate of the system and provide the maximum diversity order.

The sum rate capacity of the multi-user MIMO uplink system is achieved via an MMSE receiver with successive interference cancellation. The sum-rate capacity of a downlink multi-user MIMO system employing DPC and an uplink multi-user MIMO system employing successive interference cancellation is at most  $\min(N_T, K)$  times larger than the maximum achievable sum rate capacity of a system using TDMA. Motivated by small size and low power consumption of user terminals, we focus on the base station antenna spacing and user separations. This means that one user will not be aware of other users sharing the same time and frequency resources and that the base station will have the task of reducing the multi-user interference by keeping sufficient antenna spacing[18].

In this chapter we will address the problem of generalized designs and approximations of the spatial correlation and correlation matrices in an indoor multi-user MIMO communication system. The focus will be put on the multi-user MIMO downlink (MIMO-BC) and uplink (MIMO-MAC) system, since in this case most of the solutions for the downlink can be applied on the uplink in a straightforward way. Another reason for this is that by using the MU-MIMO antenna spacing and user separation on both the uplink and the downlink we can reduce the complexity at the base station. Moreover, having in mind the complexity of DPCs and their inability to combine instantaneous and long-term channel state information at the transmitter for precoding, we give preference in our investigations to the effects of antenna spacing at base station and user separations on the capacity of MU-MIMO in both Line of Site (LOS) and Non-Line of Site (NLOS) indoor environment.

Channel state information at the transmitter allows us to exploit the benefits of having multiple antennas at the base station and the user terminals to the maximum. Channel state information can be acquired at the transmitter either if a feedback channel is present or when the transmitter and receiver operate in time division duplex (TDD) so that time-invariant MIMO channel transfer functions is the same in both ways. The cost of acquiring the channel state information at the transmitter is much lower in a TDD system, where it is possible to exploit the estimated uplink channel for the downlink transmission due to the reciprocity principle than in a frequency division duplex (FDD) system, where we have to rely on the feedback of the channel state information[18].

On the downlink the base station will use any channel state information available to mitigate or ideally completely eliminate multi-user interference through linear or nonlinear (DPC or THP) precoding, which leads to significant information rate gains. The user terminal estimates the effective channel and transmits data in the next uplink frame. The effective channel is equal to the combined network channel after the precoding at the base station.

However, on the uplink the base station has the possibility to use successive interference cancellation, so the effective channel on the uplink that includes the spatial processing does not have to be the same as on the downlink. The diversity gains of MIMO are more desirable than spatial multiplexing gains if we take into account the limited power available at the user terminal and therefore it is enough that the base station transmits to the user terminal only the dominant singular vector of the uplink effective channel[18].

## 3.2 Channel State Information

In wireless communication, channel state information (CSI) simply represents the properties of a communication link between the transmitter and receiver. The CSI describes how a signal propagates from the transmitter to the receiver and represents the combined effect of, for example, scattering, fading, and power decay with distance. The CSI makes it possible to adapt transmissions to current channel conditions, which is crucial for achieving reliable communication with high data rates in multi antenna systems [3].

The channel state information (CSI) at the transmitter is vital in MIMO systems in order to increase the transmission rate, to enhance coverage, to improve spectral efficiency and to reduce receiver complexity [3]. The CSI is usually estimated at the receiving end and then quantized and fed back to the transmitting side. Basically there are two ways that the transmitter can obtain CSI from the receiving end. The transmitter and receiver can have different CSI.

There are basically two levels of CSI, namely instantaneous CSI and statistical CSI. The following section describes both, the instantaneous and statistical CSI.

### 3.2.1 Instantaneous CSI

Instantaneous CSI is also known as short-term CSI. Instantaneous CSI means that the current conditions of the channel are known, which can be viewed as know-



ing the impulse response of a digital filter [16]. This gives an opportunity to adapt the transmitted signal to the impulse response and thereby optimize the received signal for spatial multiplexing or to achieve low bit error rates.

### 3.2.2 Statistical CSI

Statistical CSI is also known as long-term CSI. Statistical CSI means that a statistical characterization of the channel is known. This description can include the type of fading distribution, the average channel gain, the line-of-sight component, and the spatial correlation [16]. As with instantaneous CSI, this information can be used for transmission optimization.

The CSI acquisition is practically limited by how fast the channel conditions are changing. In fast fading systems where channel conditions vary rapidly under the transmission of a single information symbol, only statistical CSI is reasonable. On the other hand, in slow fading systems instantaneous CSI can be estimated with reasonable accuracy and used for transmission adaptation for some time before being outdated. In practical systems, the available CSI often lies in between these two levels; instantaneous CSI with some estimation/quantization error is combined with statistical information [16].

The capacity of a MIMO (multi-input multi-output) channel is influenced by the degree of CSI (channel-state information) available to both transmitter and receiver [2]. In most instances of multi-antenna communication, the receiver can accurately track the instantaneous state of the channel from pilot signals that are typically embedded within the transmissions. In terms of CSI at the transmitter, on the other hand, several scenarios are possible: In a narrowband flat-fading channel with multiple transmit and receive antennas (MIMO), the system is modeled as

$$y = H.x + n \tag{3.1}$$

where  $y$  and  $x$  are receive and transmit vectors, respectively.  $H$  and  $n$  are the channel matrix and the noise vector, respectively. Let us suppose the noise is modeled as circular symmetric complex normal with

$$n \sim CN(0, S) \tag{3.2}$$

where the mean value is zero and the noise covariance matrix  $S$  is known.

- Instantaneous CSI Ideally, the channel matrix  $H$  is known perfectly. Due to

channel estimation errors, the channel information can be represented as

$$Vec(H_{estimate}) \sim CN(Vec(H), R_{error}) \quad (3.3)$$

where  $H_{estimate}$  is the channel estimate and  $R_{error}$  is the estimation error covariance matrix. The vectorization  $vec()$  was used to achieve the column stacking of  $H$ , as multivariate random variables are usually defined as vectors.

- **Statistical CSI** In this case, the statistics of  $H$  are known. In a Rayleigh fading channel, this corresponds to knowing that

$$Vec(H) \sim CN(0, R) \quad (3.4)$$

for some known channel covariance matrix  $R$ . Correlation matrix  $R$  is the expectation of vectorized  $H$  channel matrix with its Hermitian conjugate [16].

$$R = E[vec(H)vec(H)^\dagger] \quad (3.5)$$

### 3.3 Antenna Spacing and Correlations

Antennas are a very important component of communication systems. By definition, an antenna is a device used to transform an RF signal traveling on a conductor into an electromagnetic wave in free space. Antennas demonstrate a property known as reciprocity, which means that an antenna will maintain the same characteristics regardless if it is transmitting or receiving. Most antennas are resonant devices, which operate efficiently over a relatively narrow frequency band. An antenna must be tuned to the same frequency band of the radio system to which it is connected; otherwise the reception and the transmission will be impaired. When a signal is fed into an antenna, the antenna will emit radiation distributed in space in a certain way. A graphical representation of the relative distribution of the radiated power in space is called a radiation pattern [27].

#### 3.3.1 Antenna Radiation Pattern

The radiation pattern or antenna pattern is the graphical representation of the radiation properties of the antenna as a function of space [27]. That is, the antennas pattern describes how the antenna radiates energy out into space (or how it receives energy). It is important to state that an antenna radiates energy in all directions, at least to some extent, so the antenna pattern is actually three-dimensional. It is

common, however, to describe this 3D pattern with two planar patterns, called the principal plane patterns.

These principal plane patterns can be obtained by making two slices through the 3D pattern through the maximum value of the pattern or by direct measurement. It is these principal plane patterns that are commonly referred to as the antenna patterns. In discussions of principal plane patterns or even antenna patterns, you will frequently encounter the terms azimuth plane pattern and elevation plane pattern. The term azimuth is commonly found in reference to the horizon or the horizontal whereas the term elevation commonly refers to the vertical. When used to describe antenna patterns, these terms assume that the antenna is mounted (or measured) in the orientation in which it will be used [27].

### **3.3.2 Antenna Lobe**

Any given antenna pattern has portions of the pattern that are called lobes. A lobe can be a main lobe, a side lobe or a back lobe and these descriptions refer to that portion of the pattern in which the lobe appears. In general [27], a lobe is any part of the pattern that is surrounded by regions of relatively weaker radiation. So a lobe is any part of the pattern that sticks out and the names of the various types of lobes are somewhat self-explanatory.

Radiation Lobe is a clear peak in the radiation intensity surrounded by regions of weaker radiation intensity. Main Lobe (major lobe, main beam) is radiation lobe in the direction of maximum radiation. Minor Lobe is any radiation lobe other than the main lobe. Side Lobe is a radiation lobe in any direction other than the direction(s) of intended radiation. Back Lobe is the radiation lobe opposite to the main lobe. Half-Power Beamwidth (HPBW) is the angular width of the main beam at the half-power points. First Null Beamwidth (FNBW) is angular width between the first nulls on either side of the main beam [27].

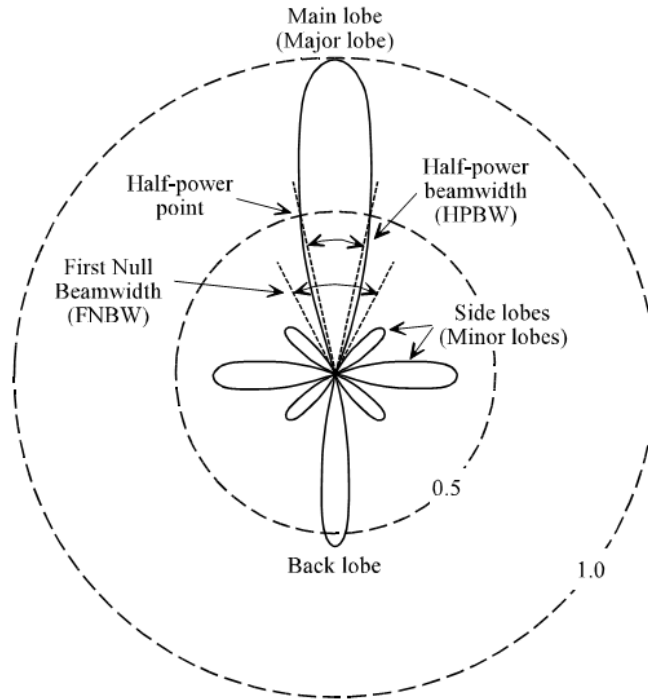


Figure 3.1: Antenna Pattern Parameters [27]

### 3.3.3 Grating Lobes in Antenna Arrays

Another phenomenon associated with phased array probes is the generation of unwanted grating lobes or side lobes, two closely related phenomena caused by sound energy that spreads out from the transducer at angles other than the primary path. This phenomenon is not limited to phased array systems. This unwanted lobe also occurs with conventional transducers as element size increases. These unwanted ray paths can reflect off surfaces in the test piece and cause spurious indications on an image. The amplitude of grating lobes is significantly affected by pitch size, the number of elements, frequency, and bandwidth.

Grating lobes will occur whenever the size of individual elements in an array is equal to or greater than the wavelength, and there will be no grating lobes when element size is smaller than half a wavelength [27]. (For element sizes between one-half and one wavelength, the generation of grating lobes will depend on the steering angle.) Thus the simplest way to minimize grating lobes in a given application is to use a transducer with a small pitch. Specialized transducer design incorporating subdicing (cutting elements into smaller elements) and varying element spacing will also reduce unwanted lobes.

### 3.4 Uplink-Multiple Access Multiuser-MIMO

Under this topic, we consider a K-user MIMO system over a flat fading MAC with  $M$  antennas at BS and single antenna at each UE. Denote  $H_K$  and  $X_K$  the channel matrix and the transmitted vector of UE  $K$ . The received vector from  $K$  user  $y$  in [2, 18] is

$$y = \sum_{k=1}^K H_K X_K + n \quad (3.6)$$

Where  $n$  is a vector of complex additive white Gaussian noise (AWGN) samples with zero mean and unit variance.  $H_K$  in (3.6) are independent among different UE's and perfectly known at both the transmitter and the receiver.

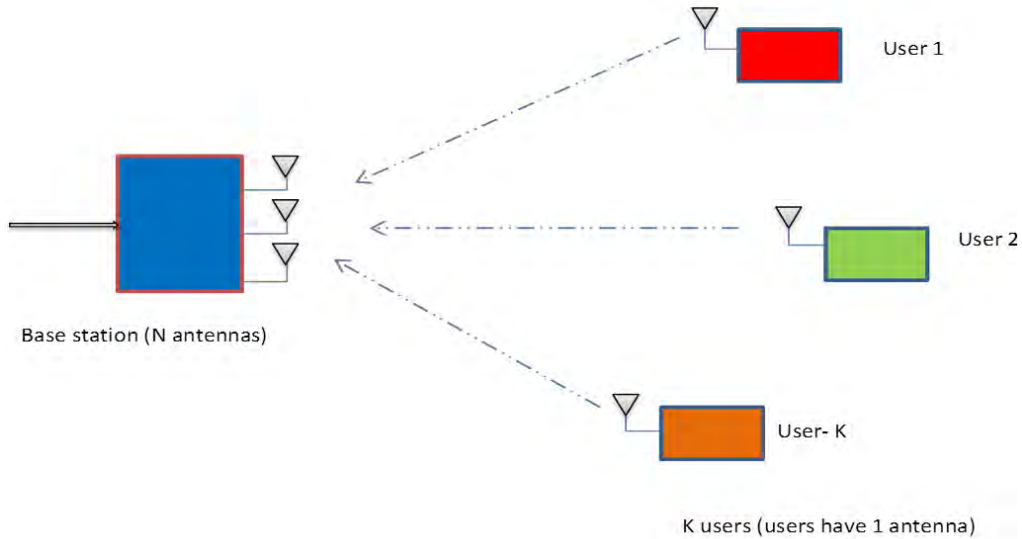


Figure 3.2: MIMO-MAC with single antenna users

Following the common Kronecker channel correlation model for indoor NLOS, we can write  $H_K$  as

$$H_K = \sqrt{R_{RX}} H_W \sqrt{R_{TX}} \quad (3.7)$$

Where  $H_W$  is a Rayleigh fading matrix whose entries is independent and identically distributed complex circular symmetric Gaussian variables with zero mean and unit variance. And  $R_{TX}$ ,  $R_{RX}$  in (3.7) are semi-positive definite matrices that characterize correlation effects of antennas at the transmitter and the receiver respectively for the link between K-UE and the BS. Following [2, 18] the common Kronecker channel correlation model for indoor LOS, we can write  $H_K$  as

$$H_K = \sqrt{R_{RX}} H_z \sqrt{R_{TX}} \quad (3.8)$$

Where  $H_z$  a Gaussian matrix is whose entries is independent and identically distributed with zero mean and unit variance. And similarly,  $R_{RX}$  and  $R_{RX}$  in (3.8) are semi-positive definite matrices that characterize correlation effects of antennas at the transmitter and the receiver respectively for the link between K-UE and the BS. Where the sum-rate capacity in MACs under individual power constraints for each channel can be formulated in [see: **Appendix-A**] as

$$C_{MAC} = \left( \max_{tr(\sum_{k=1}^K Q_K) \leq P_K} \right) \log_2 \det \left( I_M + \sum_{K=1}^K H_K Q_K H_K^* \right) \quad (3.9)$$

$$\text{Subject to } tr \left( \sum_{k=1}^K Q_K \right) \leq P_K, \forall K.$$

where  $Q_K = E[X_K X_K^*]$  and  $P_K$  are input covariance matrix and the maximum transmitted power of K-UE, respectively. It is well known that the spatial correlation between two adjacent identical antennas due to the arrival of a single plane wave can be approximated as in (2.23) a Jakes correlation function of its incident angle,  $\Phi$ , as

$$\rho(d) = e^{-j2\pi \frac{d}{\lambda} \cos(\Phi)} \quad (3.10)$$

where  $d$  is the antenna separation,  $\lambda$  is the carrier frequency wavelength and  $\Phi$  is the angle of departure (AOD) at the transmitter and angle arrival (AOA) at the receiver spread [18]. And assumed to be 45 degree angle of departure (AOD) at the transmitter and angle arrival (AOA) at the receiver spread in LOS and 10 degree angle of departure (AOD) at the transmitter and 22.5 degree angle of arrival (AOA) at the receiver spread in NLOS. As we can see in (3.10) the correlation coefficient is the function of antenna separation only. The matrix  $R_{TX}, R_{RX}$  is complex exponential correlation model characterized by

$$R_{Tx}, R_{Rx} = \begin{bmatrix} 1 & \rho^* & \dots & \rho^{*(N-1)} \\ \rho & 1 & \dots & \rho^{*(N-2)} \\ \vdots & \vdots & \ddots & \vdots \\ \rho^{(N-1)} & \rho^{(N-2)} & \dots & 1 \end{bmatrix} \quad (3.11)$$

where  $N$  is equal to  $N_r$  or  $N_t$ , corresponding to the receive or transmit antenna array, and  $\rho$  is the fading correlation between two adjacent receive or transmit antenna elements. Note that for small  $\rho(d)$ , the higher-order terms are negligible and the correlation matrices take the form of diagonal matrices.

In practical cases, the degenerate channel phenomena called keyholes may arise, where the antenna elements at both the transmitter and the receiver have very low correlation, yet the channel matrix  $H$  has only a single degree of freedom, yielding a single mode of communication [2]. This phenomenon is very similar to the case

when rich-scattering transmit and receive antennas are separated by a screen with the wave passing through a keyhole. This model also applies for indoor propagation through hallways, narrow tunnels or wave guides. Relay channels in the amplify-and-forward mode can be treated as keyhole channels. Thus, low correlation is not a guarantee for achieving high capacity.

### 3.5 Downlink-Broadcasting Multiuser-MIMO

We still use  $K$  and  $M$  to denote the number of UEs in the system, and the number of antennas at the BS respectively. As we can see from Figure 3.3 below, a single base station with multiple antennas broadcasting signals to UE with single antenna element. At the BS we assumed uniform linear array (ULA) which is the most common linear antenna array.

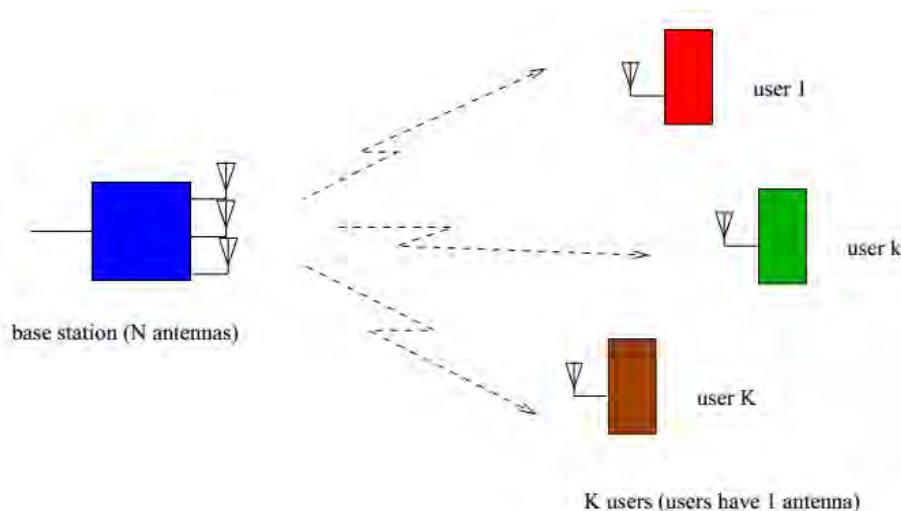


Figure 3.3: MIMO-BC with M antenna base stations

Denote  $H_K$  the channel matrix between the BS and K-UE. The received vector  $y_K$  at K-UE can be written [2, 18] and [28] as

$$y_K = H_K X + n_K \quad (3.12)$$

where,  $X$  is the transmitted vector of the BS and  $n_K$  is a vector of complex AWGN samples with zero mean and unit variance. Similar to the MAC,  $H_K$  are independent among all UEs and perfectly known at both the transmitter and the receiver sides. The common Kronecker channel correlation model in (3.7) and (3.8) are still used. Note that in this case,  $R_{TX}$  and  $R_{RX}$  with  $tr(R_{TX}) = M$  and  $tr(R_{RX}) = K$  represent correlation effects at the BS side and K-UE side respectively. Based on the duality

principle between MIMO BCs and MACs shown in [see: **Appendix-A**], the sum-rate capacity of a BC can be written as

$$C_{BC} = \left( \max_{tr(Q_K) \leq P} \right) \log_2 \det \left( I_R + \sum_{K=1}^K H_K^* Q_K H_K \right) \quad (3.13)$$

Subject to  $tr(Q_K) \leq P$ .

where,  $P$  is the transmitted sum power constraint for the BS and  $Q_K$  the input covariance matrix of K-UE in the dual MAC. Note that the difference between equation (3.9) and (3.14) is the power constraint. The former is based on individual power constraints; while the later is based on a sum power constraint.

### 3.6 Indoor Scenario Consideration

As we have mentioned earlier in this thesis work, our work is mainly studied for indoor scenario. Based on indoor environment we divided into three scenarios which is reliant on the location of UE and AP (BS) when both are LOS, NLOS and both LOS and NLOS to each other. These are:

1. **Scenario-I:** when BS and MS are both in LOS

- We considered the channel is fixed and we assumed it as iid Gaussian non-fading channel ( $H_Z$ ) [8, 9, 10]. Therefore, the Kronecker channel correlation would becomes

$$H_{K1} = \sqrt{R_{Rx}} H_Z \sqrt{R_{Tx}} \quad (3.14)$$

- Then by duality principle of MIMO BC-MAC [see: **Appendix A**], the uplink and downlink MU-MIMO sum-rate channel capacity in LOS can be obtained by substituting equation (3.15) into equation (3.9) and (3.14).

2. **Scenario-II:** when BS and MS are both in NLOS

- In this scenario we consider the channel is variable due to multiple scatterer and we assumed the Rayleigh fading channel [13] which is iid complex symmetric Gaussian ( $H_W$ ). Therefore, the Kronecker channel correlation would become,

$$H_{K2} = \sqrt{R_{Rx}} H_W \sqrt{R_{Tx}} \quad (3.15)$$

- Then by using the duality principle of MIMO BC-MAC [see: **Appendix**



**A**], the uplink and downlink MU-MIMO sum-rate channel capacity in NLOS can be obtained by substituting equation (3.16) into equation (3.9).

3. **Scenario-III:** when BS is LOS to some users and NLOS to others,

- In this scenario we consider that the channel is fading and we assumed Ricean fading channel [13] which is the sum of fixed and variable (fading) channels when  $K$  is the constant Ricean factor. i.e.

$$H_R = \sqrt{\frac{K}{K+1}}H_{fixed} + \sqrt{\frac{1}{K+1}}H_{variable} \quad (3.16)$$

- Therefore, in the Kronecker channel correlation would become,

$$H_{K3} = \sqrt{R_{Rx}}H_R\sqrt{R_{Tx}} \quad (3.17)$$

- Then similar to the above two scenarios, by using duality principles of MIMO BC-MAC [see: **Appendix A**], we can obtain the sum-rate channel capacity in both LOS an NLOS by substituting equation (3.18) into equation (3.9) and (3.14).

The following table contains the assumed indoor LOS and NLOS antenna correlation in both uplink(MIMO-MAC) and downlink(MIMO-BC) and the Kronecker model.

Table 3.1: Indoor correlation matrix

Correlation matrix	Uplink(MIMO-MAC)	Downlink(MIMO-BC)
$R_{Tx}$	$R_{MS} \rightarrow LOS$	$R_{BS} \rightarrow LOS$
	$R_{MS} \rightarrow NLOS$	$R_{BS} \rightarrow NLOS$
$R_{Rx}$	$R_{BS} \rightarrow LOS$	$R_{MS} \rightarrow LOS$
	$R_{BS} \rightarrow NLOS$	$R_{MS} \rightarrow NLOS$
$R_H$	$R_{MS} \otimes R_{BS} \rightarrow LOS$	$R_{BS} \otimes R_{MS} \rightarrow LOS$
	$R_{MS} \otimes R_{BS} \rightarrow NLOS$	$R_{BS} \otimes R_{MS} \rightarrow NLOS$

# Chapter 4

## Simulation Result and Discussion

### 4.1 Introduction

In chapter two covers some theoretical and analytical part which helps to understand this thesis work and in chapter three, Jakes spatial correlation model and Kronecker channel correlation model was discussed. And also, MU-MIMO channel capacity based on duality principles of MIMO-MAC and MIMO-BC which differs based on their power constraints was discussed. In this chapter, demonstration of simulation results on the basis of ideas discussed in previous two chapters using MATLAB 13.0 is going to be done.

It is obvious that, nowadays thanks to technology we have a lot of programming languages and coding platforms available for system simulation development including C/C++, Java, MATLAB, atoll and other modeling software. While the first two offer much faster execution of the program, they require developing libraries or components for each and every element, which is very time consuming. Sometimes, open source libraries for different functions are available, but their reliability is not guaranteed and also atoll like modeling packages can model a system but based on pre-defined inbuilt formulas algorithms which are not modified or changed.

On the other hand, MATLAB is relatively slow in terms of execution speeds but has numerous built-in functions and specially developed tool boxes for communications and signal processing which makes the coding both simple and straight forward. Since the focus of this thesis is not developing new basic tools, but rather using those tools for evaluations purposes, these built-in functions save significant time and energy. Also, the powerful computers can run the system at a reasonably fast pace, so for this reason, MATLAB has been chosen as the underlying platform for all simulator and code development work.

For comparison one must take note that MIMO-MAC channel capacity, MIMO-BC channel capacity is based on antenna spacing, user separation and fading model. In order to present equitable comparison, we assume that in MIMO-BC the total transmitted power is equally allocated among antenna elements at BS and in MIMO-MAC case the transmitted power is based on individual power constraints. And also, the channel state information (CSI) at both transmitter and receiver side is assumed to be known. Angle of spread and angle of incidence is taken based on the BS and Users location in indoor scenarios.

Table 4.1: Simulation parameters

Antenna spacing at BS	From $0.1\lambda$ up to $1\lambda$
User separation in LOS and NLOS	From 0.5m up to 10m in LOS From 2m up to 30m in NLOS
Angle of Departure, Angle of Arrival	Both 45 degree in LOS 10 degree and 22.5 degree in NLOS respectively
Spatial Correlation	Jakes spatial correlation model
Channel Correlation	Kronecker channel correlation model
Channel model	iid non-fading Gaussian channel for indoor LOS Rayleigh fading channel for indoor NLOS Ricean fading channel for indoor LOS and NLOS
Transmit power	Equally distributed among all antennas at BS Based on individual power constraints at MS
Carrier frequency	2.4GHz
Channel State Information	Known both at transmitter and receiver side

## 4.2 Flow Chart

It is essential to visualize the simulation using flow chart since it describes the ones understanding of the whole process easily and it also gives a chance to think where the process can be improved .Flow chart is shown in Figure 4.1 below.

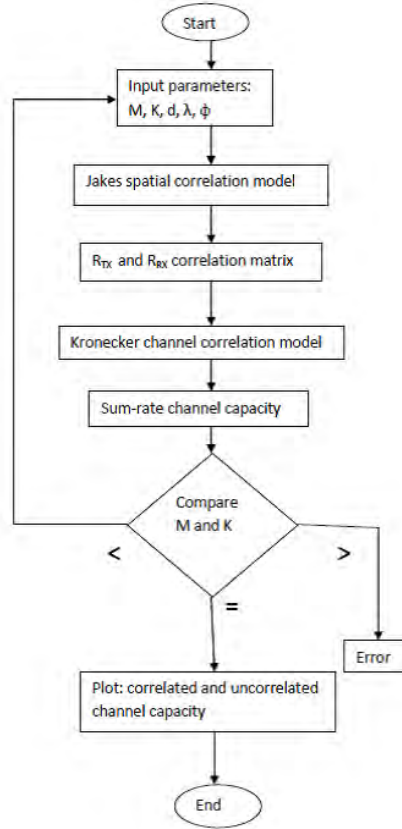


Figure 4.1: Simulation flow chart

## 4.3 Antenna Spatial Correlation

Suppose we have  $M$  antenna at BS and  $K$  mobile User in an indoor environment, then the antenna correlation is the interference between adjacent antenna elements during broadcasting of the same signal to  $K$  users and multi-cast of different message signal for  $K$  users simultaneously. Normally spatial correlation is small number from 0 to 1. It is easy to achieve sufficient antenna spacing and very small spatial correlation by varying the space between adjacent antenna elements without wasting transmission power and bandwidth. However, in modern wireless technology, it is challenging to increase the spacing between adjacent antenna elements as we like because of modern wireless equipment size. But, it is possible to obtain adequate

antenna spacing to get optimum channel capacity.

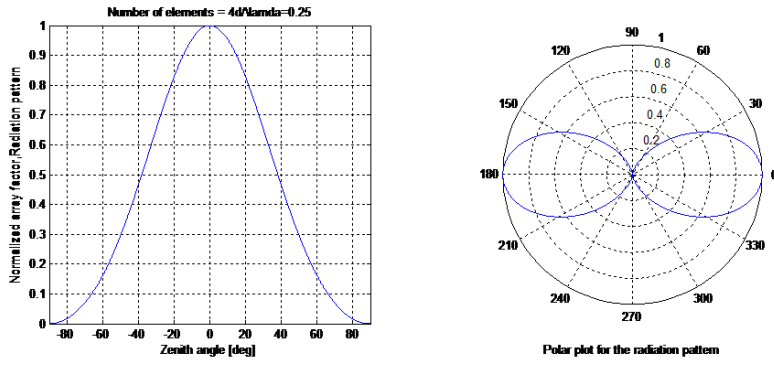
## 4.4 Channel Capacity

Channel capacity is the upper limit of transmission rate for reliable communication. Channel capacity depends on signal to noise ratio (SNR), number of antenna elements (in MU-MIMO) and bandwidth. In the next section, we will see the simulation result for the effects of antenna spacing and random user separation on correlation coefficient and channel capacity. We will also see the simulation result for MIMO-BC and MIMO-MAC channel capacity (i.e., in *bits/s/Hz*) of four transmit and four receive antenna for Rayleigh fading channel, iid Gaussian and four transmit and eight receive Ricean fading channel with an intention of comparing the amount of SNR required for the same spatial correlation of the three different channels (Rayleigh, Gaussian and Ricean fading). Since this thesis is focused to find adequate antenna spacing for optimum MU-MIMO channel capacity, by comparing the three graphs of Rayleigh, Gaussian and Ricean channel to be seen later, here it has been confirmed that Ricean fading outperforms Rayleigh fading as it has a strong signal component.

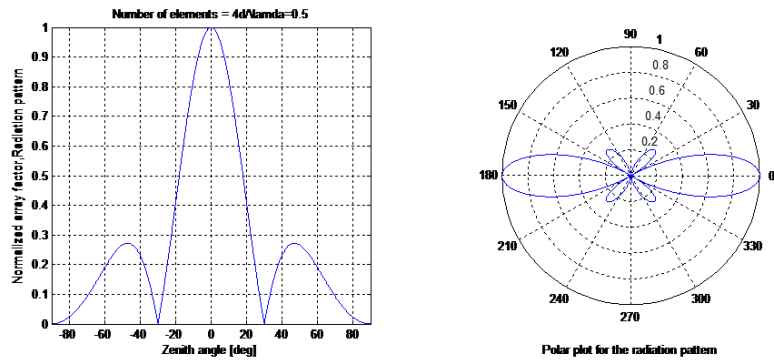
## 4.5 Simulation Results and Discussion

### 4.5.1 Antenna Radiation Pattern

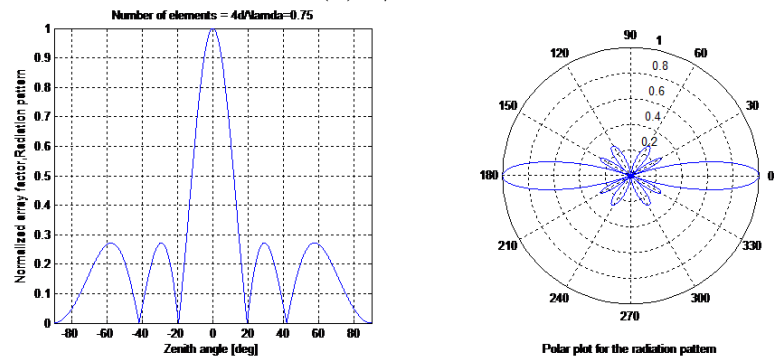
For four elements uniform linear array (ULA) antennas at BS of different spacing, [27] its radiation pattern looks like as shown in Figure 4.2 below. As we can see from Figure 4.2, as the spacing between two adjacent antenna increases from  $0.25\lambda$  to  $1\lambda$  the strength of the side-lobe also increases. This increment in side lobe strength finally leads to unintended lobe called grating lobes. The grating lobe occurs when the spacing between two adjacent antennas is  $1\lambda$  and its spreading angle is 90 degree.



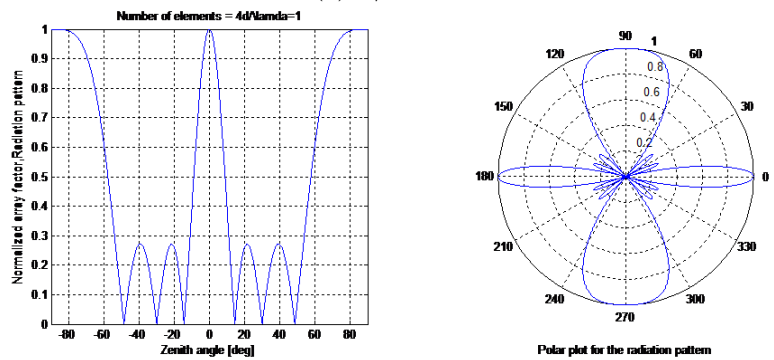
(a)  $d/\lambda = 0.25$



(b)  $d/\lambda = 0.5$



(c)  $d/\lambda = 0.75$



(d)  $d/\lambda = 1$

Figure 4.2: Antenna radiation pattern for different spacing

## 4.6 Spatial correlations

As mentioned earlier in chapter three, the spatial correlation was modeled by using Jake's spatial correlation model which is equivalent to zero order Bessel function. From this model, as the spacing between two adjacent antenna elements and the separation distance among randomly distributed k-users increases the spatial correlation of antenna decreases. Here, we can conclude that by increasing the spacing between antenna elements at BS and the separation distance between K-users we can decrease the antenna spatial correlation as shown in Figure 4.3, 4.4 and 4.5 respectively. But, with the size of latest technology devices we cannot increase the space between two adjacent antenna elements as we like. The aim of this thesis work is not to increase antenna spacing but to find the adequate spacing between two antenna elements. Here Figure 4.3 shows the effects of antenna spacing on spatial correlation from  $0.1\lambda$  to  $\lambda$  with carrier wavelength of  $0.125\text{m}$ .

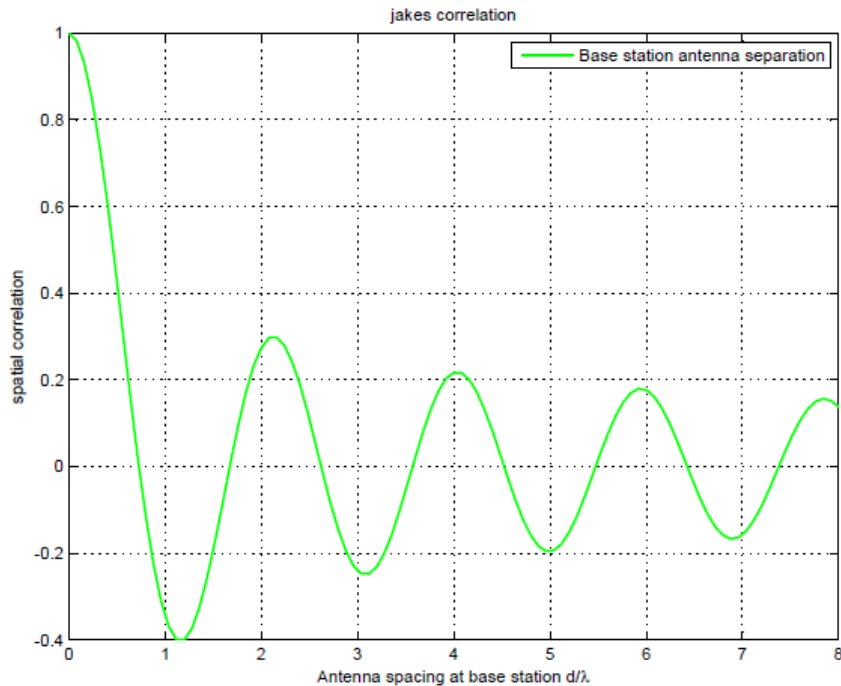


Figure 4.3: Effects of antenna spacing on spatial correlation at BS

Figure 4.4 and Figure 4.5 below shows effects of user separation on spatial correlation in LOS which is from  $0.5\text{m}$  to  $10\text{m}$  and in NLOS from  $2\text{m}$  to  $30\text{m}$ . In both cases, as separation distance between the users increases the spatial correlation coefficient decreases.

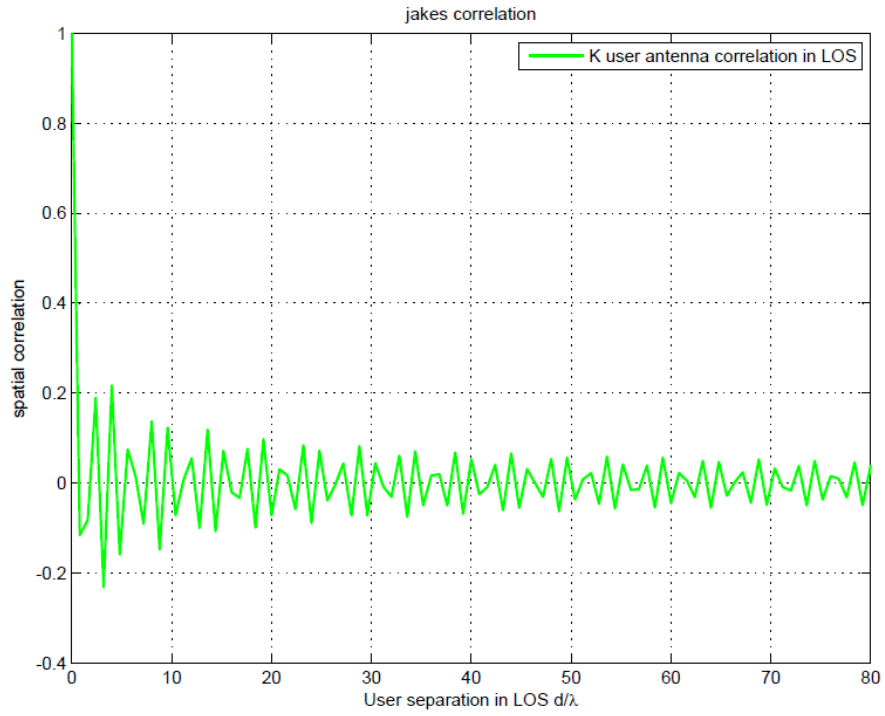


Figure 4.4: Effects of user separation in LOS on spatial correlation

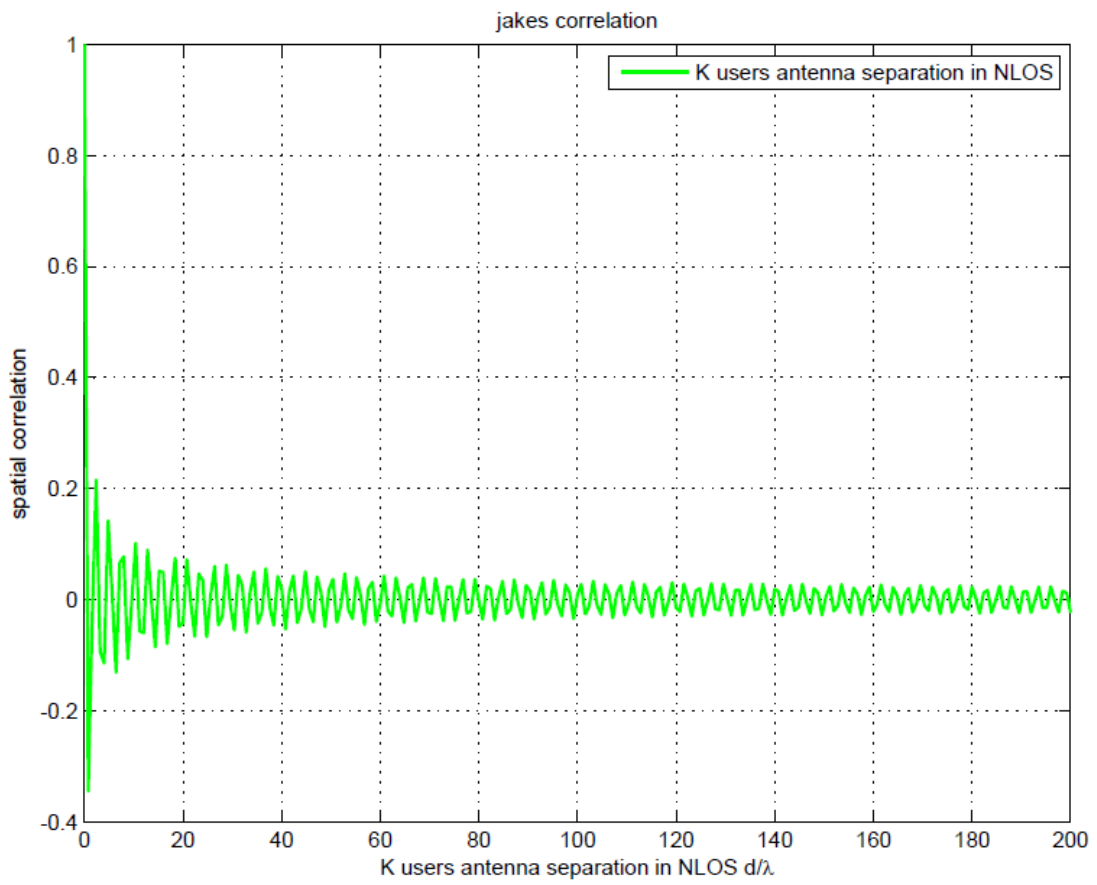


Figure 4.5: Effects of user separation in NLOS on spatial correlation



As shown in Figure 4.6 and 4.7 below, the space between two adjacent antenna elements has greater impact on indoor multiuser-MIMO BC in NLOS correlated sum-rate channel capacity as compared to uncorrelated Rayleigh fading channel. As shown below in (4xTX, 4xRX) for antenna spacing  $0.1\lambda$ ,  $0.2\lambda$ ,  $0.5\lambda$  and  $\lambda$ , the better antenna spacing could be  $0.2\lambda$  and  $0.5\lambda$  at which we can obtain better sum-rate channel capacity compared to uncorrelated Rayleigh fading channel. Here as shown by simulation, antenna spacing below  $0.2\lambda$  or above  $0.5\lambda$  minimizes the sum-rate channel capacity. So this simulation result proves again the theoretical concept which says in rich scattering environment  $0.5\lambda$  antenna spacing is sufficient. As shown in Figure 4.6 the channel capacity at  $0.1\lambda$  and  $\lambda$  are minimum compared to the uncorrelated Rayleigh fading channel capacity. The reason is at  $0.1\lambda$  the spatial correlation is high and at  $\lambda$  due to grating lobe where both parameter minimizes the channel capacity.

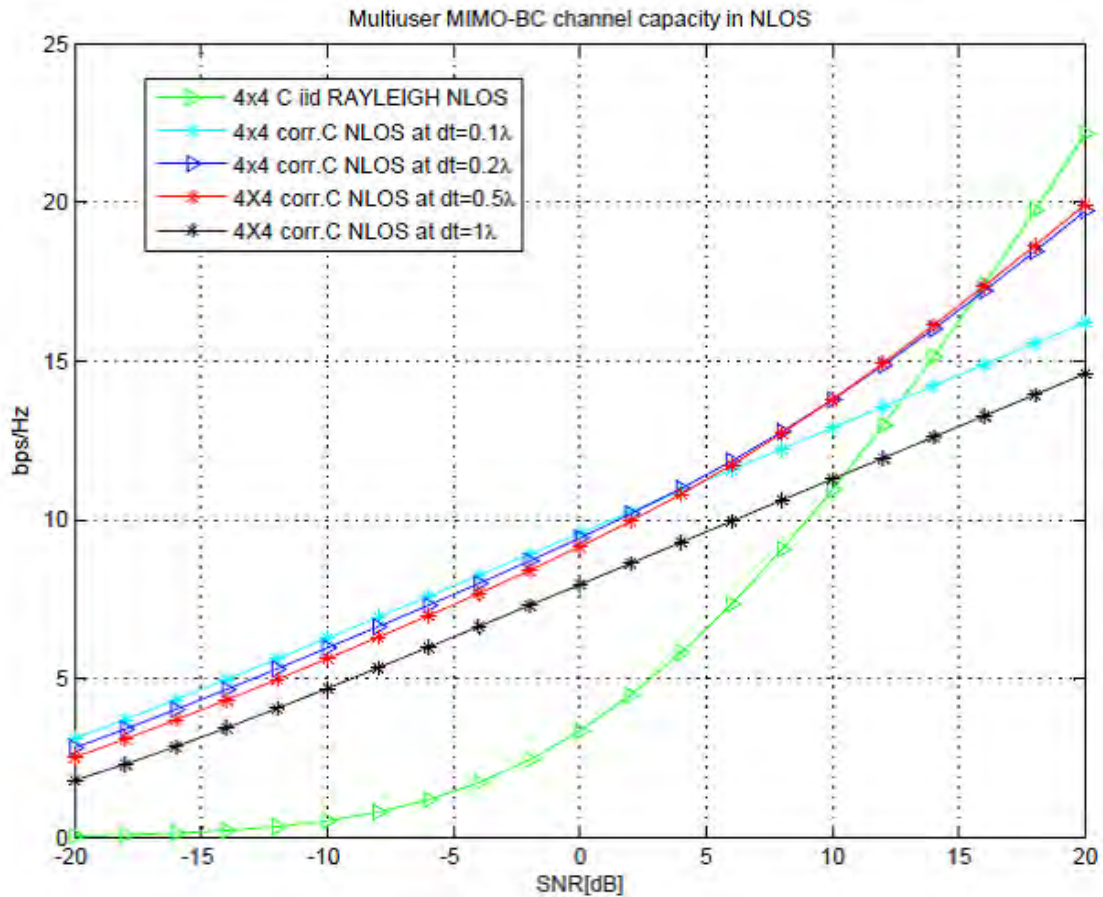


Figure 4.6: (4xTX, 4xRX) MIMO-BC Sum-rate channel capacity which shows the effect of antenna spacing below  $0.5\lambda$  as compared to iid Rayleigh fading channel capacity in indoor NLOS.

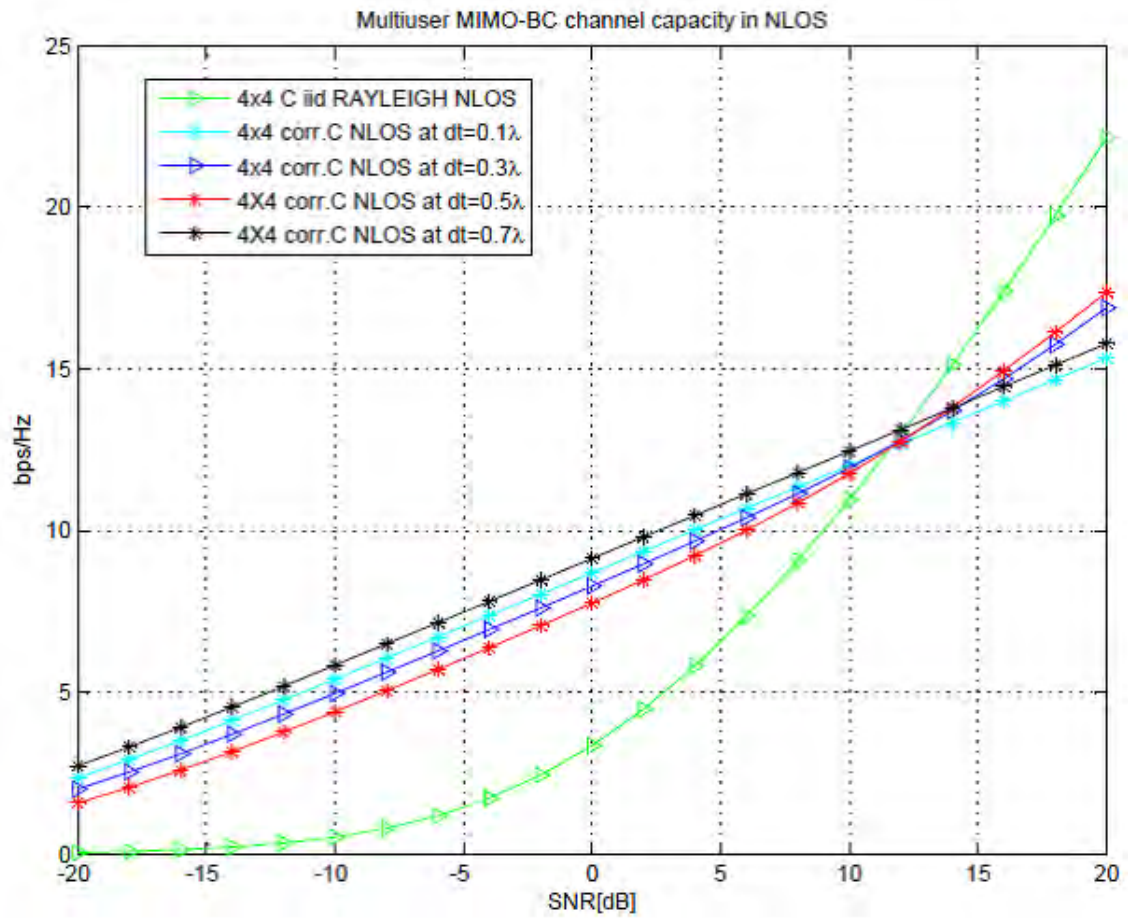


Figure 4.7: (4xTX, 4xRX) MIMO-BC Sum-rate channel capacity which shows the effect of antenna spacing above  $0.5\lambda$  as compared to iid Rayleigh fading channel capacity in indoor NLOS.

As shown in Figure 4.8 and 4.9 below, the multiuser MIMO-BC sum-rate channel capacity is compared to Gaussian iid channel capacity in an indoor LOS. Here, it is shown that the better antenna spacing in an indoor multiuser-MIMO BC LOS can be greater than or equal to  $0.5\lambda$ .

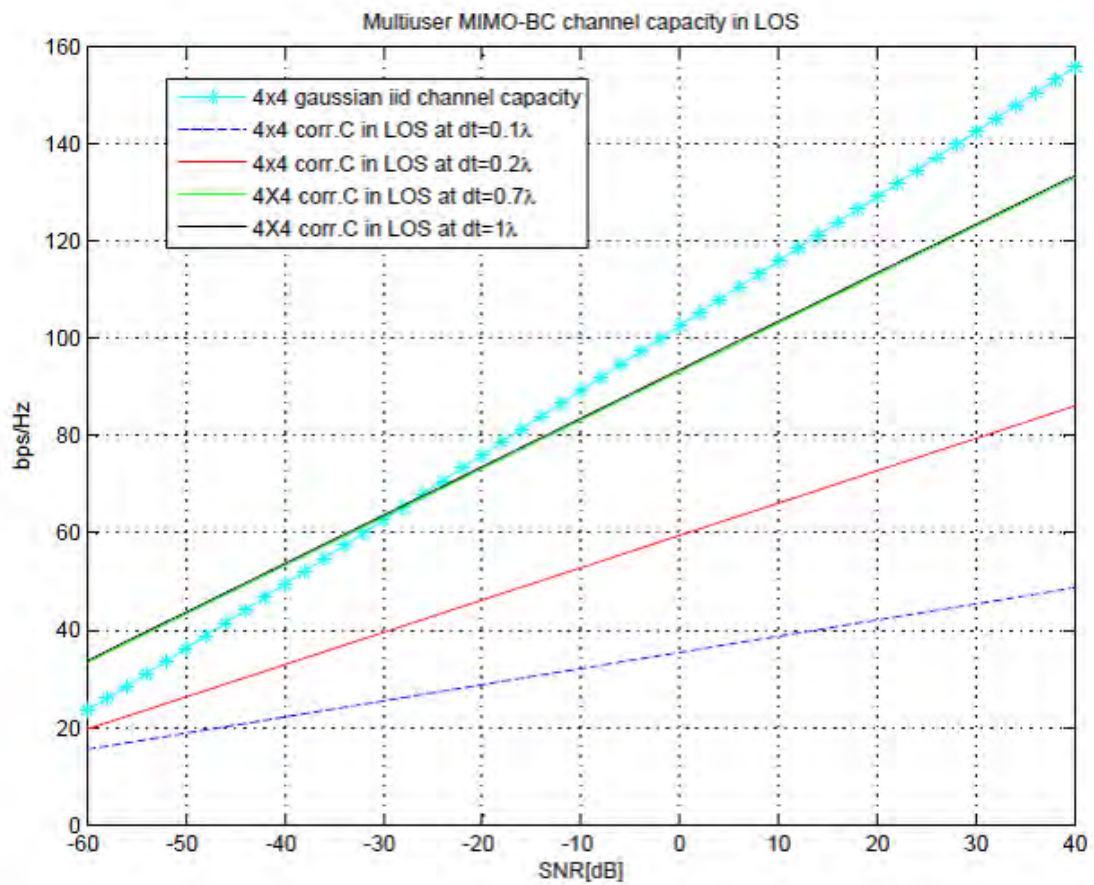


Figure 4.8: (4xTX, 4xRX) MIMO-BC Sum-rate channel capacity which shows the effect of antenna spacing above  $0.5\lambda$  as compared to Gaussian iid channel capacity in indoor LOS.

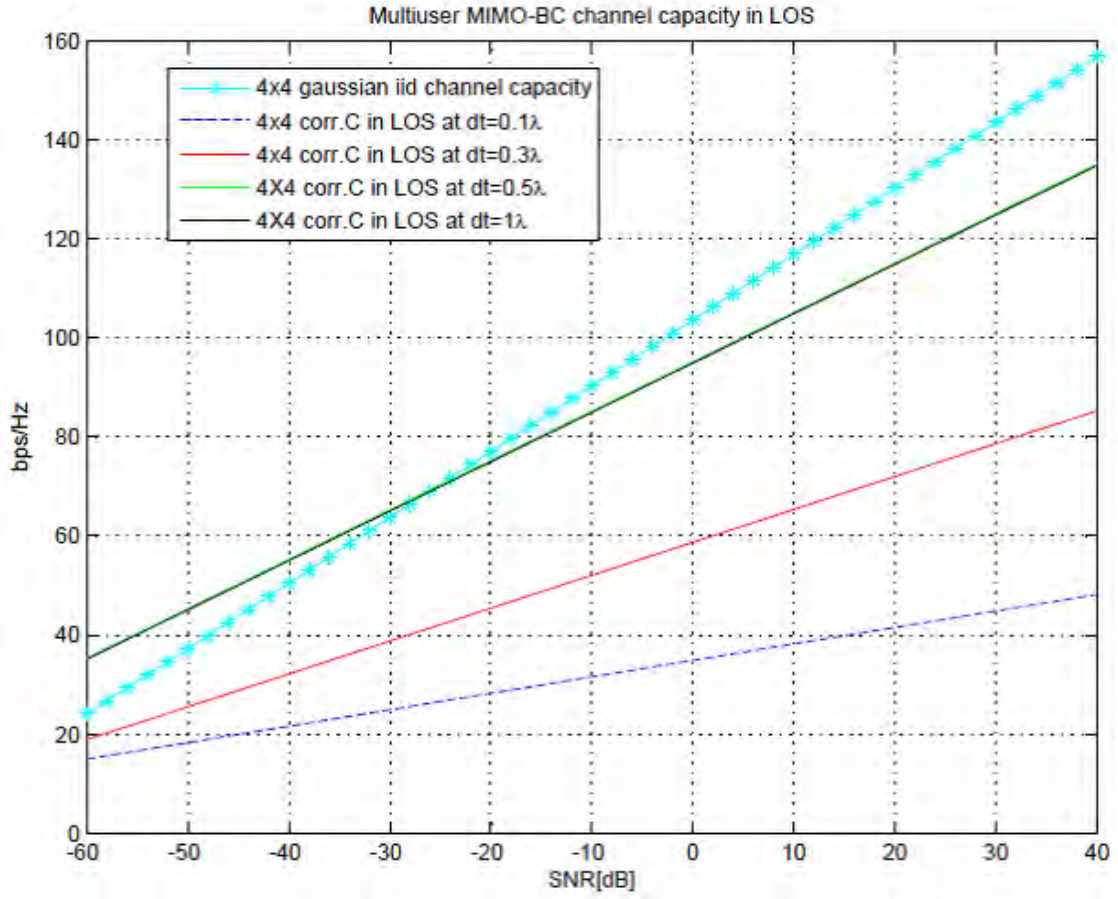


Figure 4.9: (4xTX, 4xRX) MIMO-BC Sum-rate channel capacity which shows the effect of antenna spacing below  $0.5\lambda$  as compared to Gaussian iid channel capacity in indoor LOS.

The simulation result shown in Figure 4.10 and 4.11 below indicates the effects of average random user separation distance from 0.5m to 10m in LOS and 2m to 30m in NLOS respectively. From this simulation result, as it is shown if the separation distance between the randomly distributed users is too much closer or too much far from each other it has its own impact on indoor multiuser-MIMO MAC in NLOS.

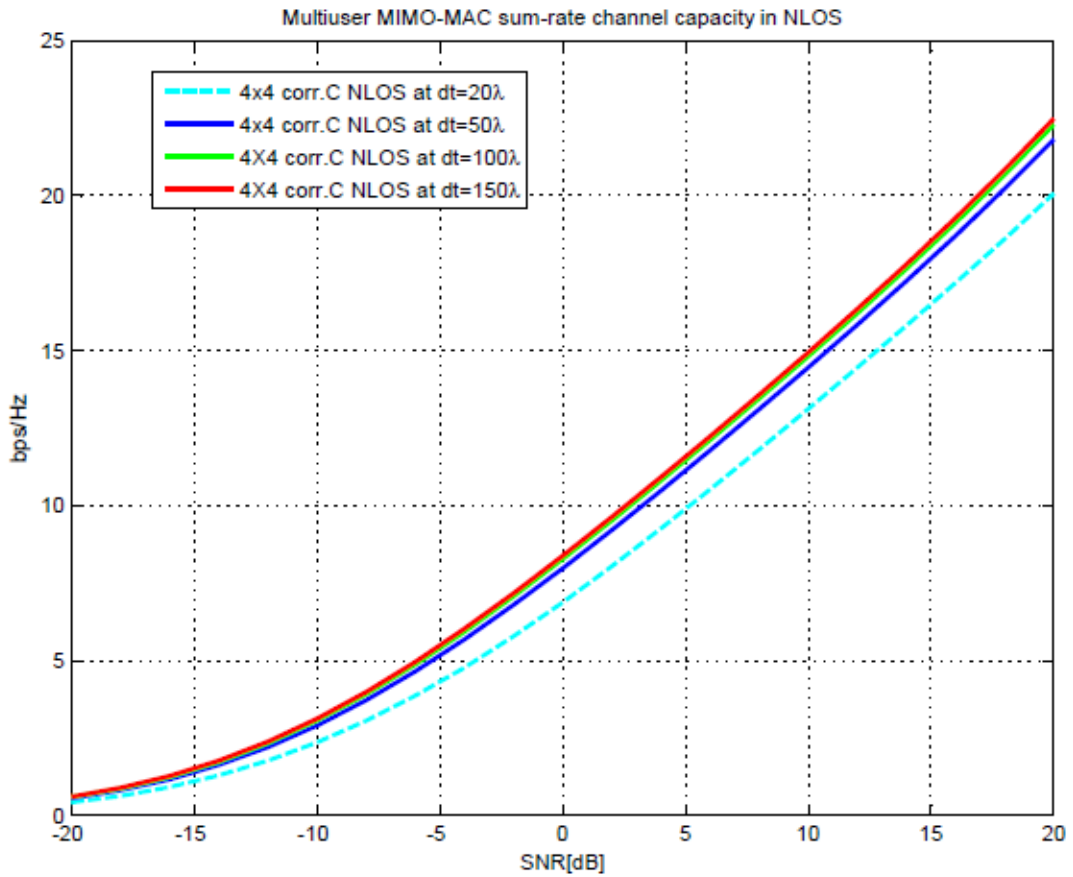


Figure 4.10: (4xTX, 4xRX) MIMO-MAC Sum-rate channel capacity which shows the effect average separation distance of sparsely randomly distributed users in 25m coverage areas in and indoor NLOS.

The Figure 4.11 below shows the effects of randomly distributed users separation distance from 0.5m to 10m in indoor multiuser-MIMO MAC sum-rate channel capacity in LOS to BS. As shown from the simulation result in MIMO-MAC if users are LOS to the BS they must not be closer to each other.

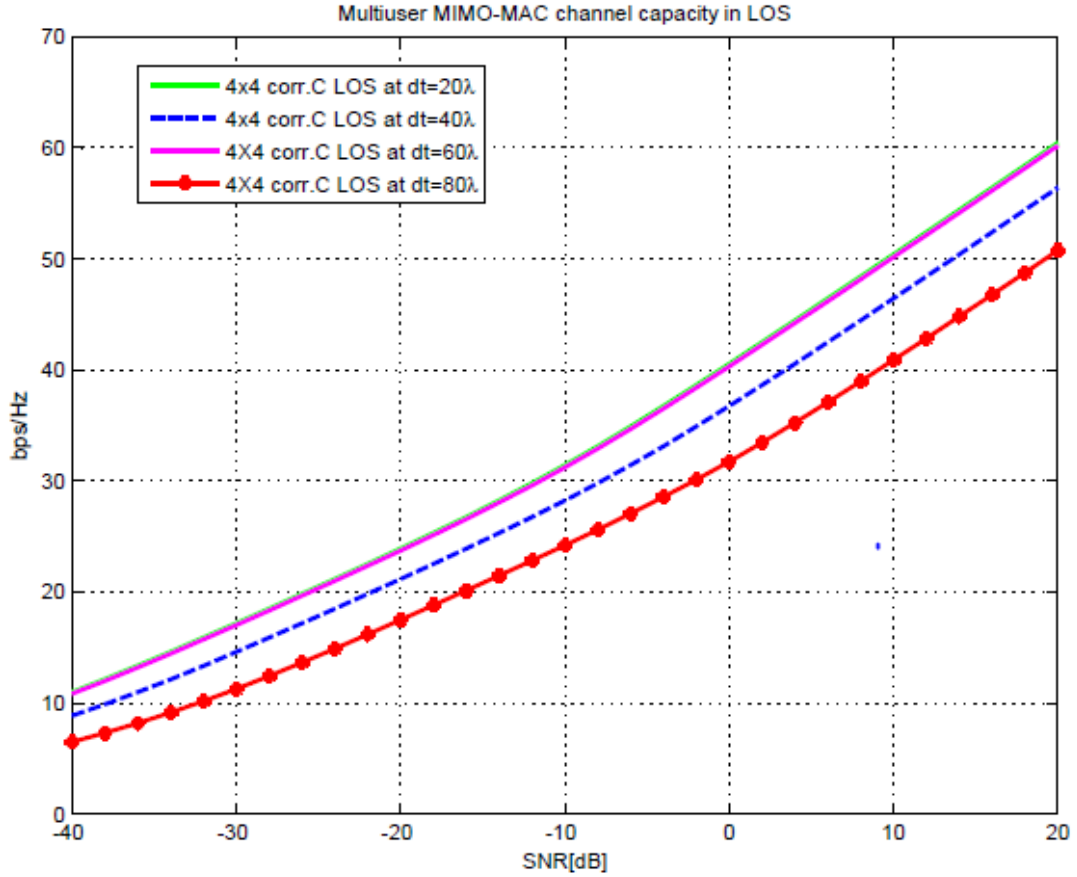


Figure 4.11: (4xTX, 4xRX) MIMO-MAC Sum-rate channel capacity which shows the effect average separation distance of randomly distributed users in 10m coverage areas in an indoor LOS.

The following simulation result shown in Figure 4.12 and 4.13, shows the effects of two adjacent antennas spacing on indoor multiuser-MIMO BC sum-rate channel capacity when users are both in LOS and NLOS to the BS. Antenna spacing for  $0.1\lambda$ ,  $0.2\lambda$ ,  $0.3\lambda$ ,  $0.5\lambda$ , and  $\lambda$  is selected. From this result we can conclude that antenna spacing above  $0.5\lambda$  is better when compared to uncorrelated Ricean fading channels.



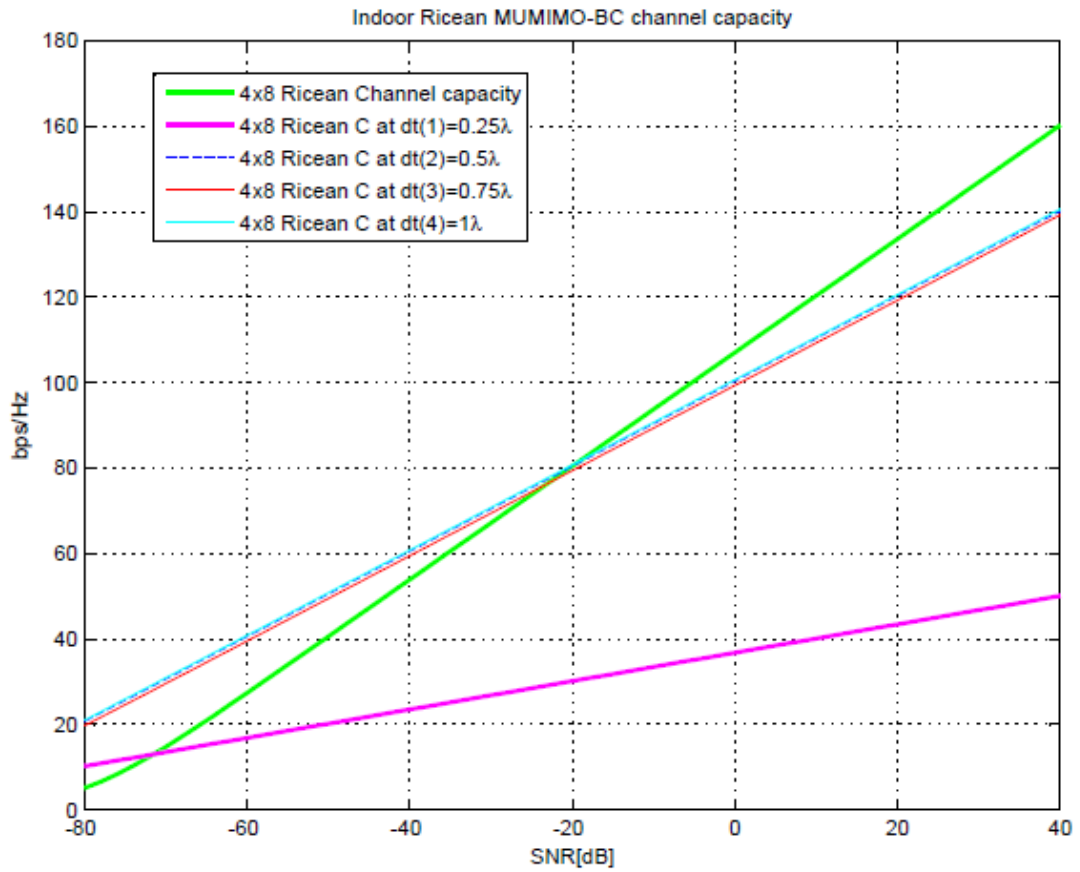


Figure 4.12: (4xTX, 8xRX) MIMO-BC Sum-rate channel capacity which shows the effects antenna spacing below and above  $0.5\lambda$  in indoor scenarios.

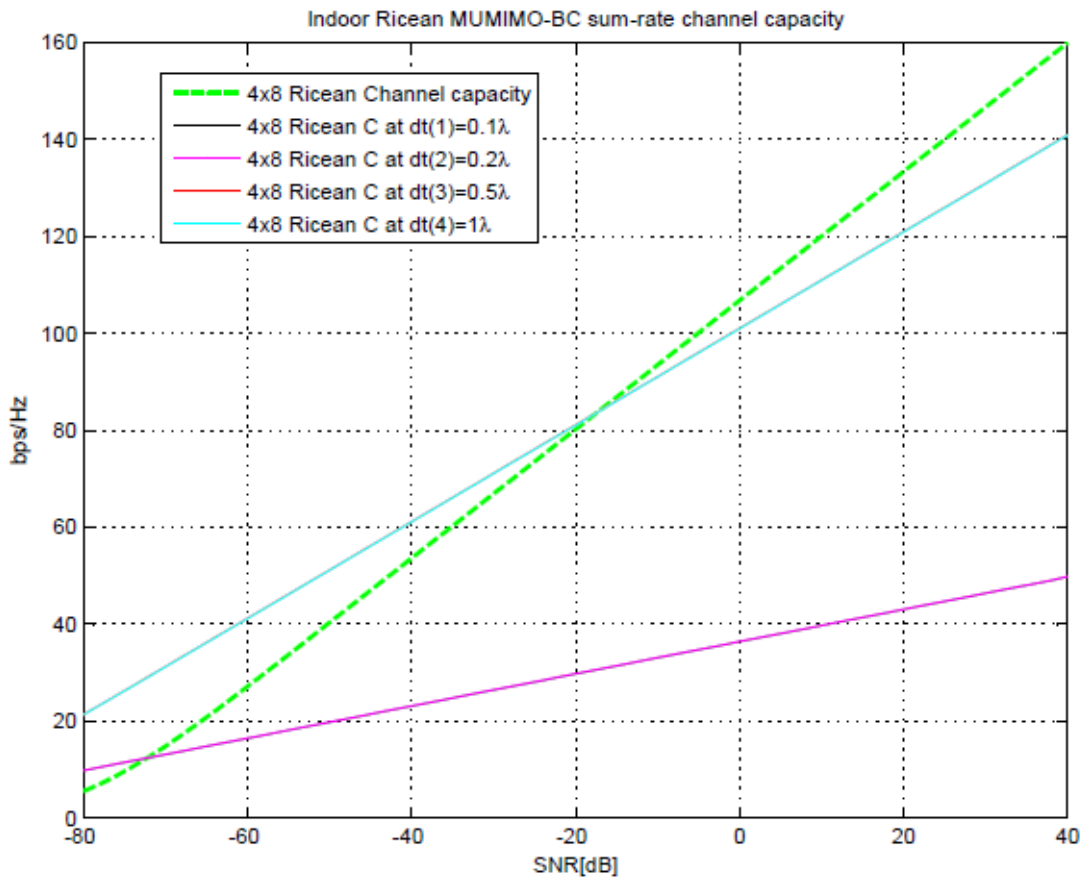


Figure 4.13: (4xTX, 8xRX) MIMO-BC Sum-rate channel capacity which shows the effects antenna spacing below and above  $0.5\lambda$  in indoor scenarios.

In the following simulation result in Figure 4.14 shows that the sum-rate channels capacity of 8-users communicating with single BS of 4-antennas using Ricean fading channel. Where  $dt(n)$  represents the random user separation distance in LOS and  $dT(n)$  represents the random user separation in NLOS.



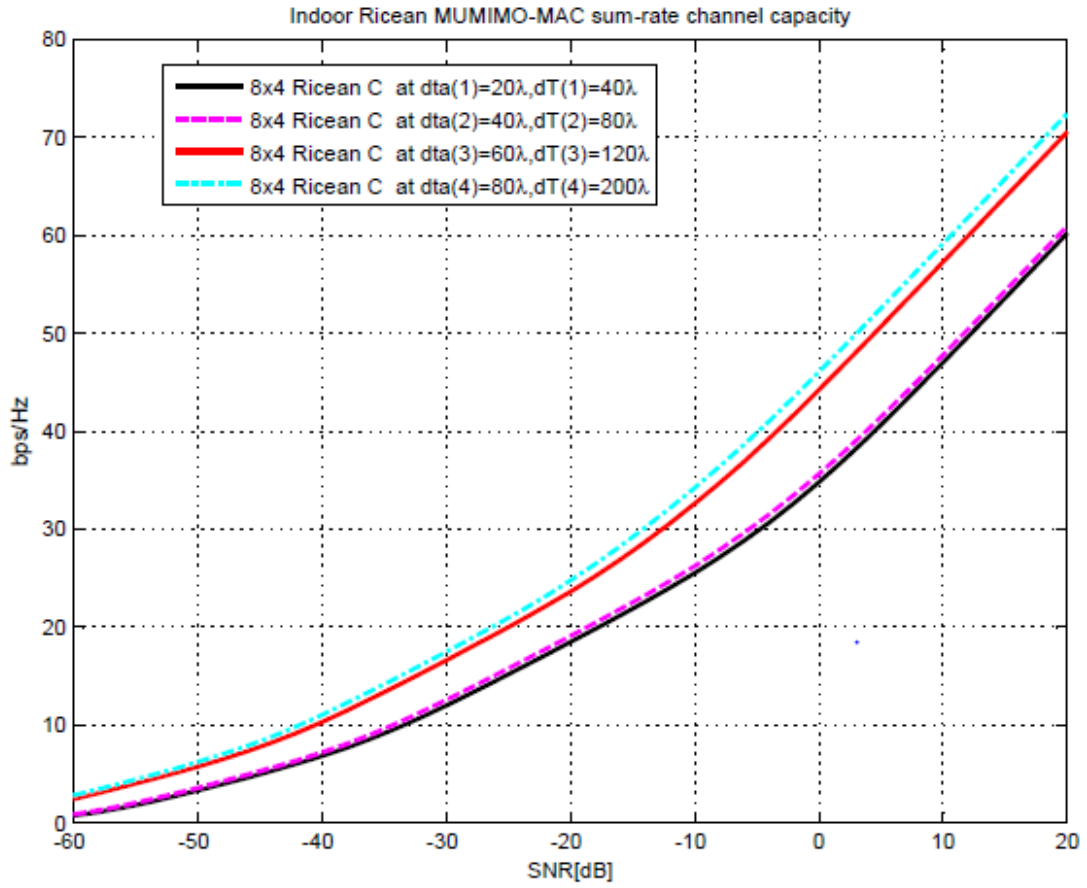


Figure 4.14: (8xTX, 4xRX) MIMO-MAC Sum-rate channel capacity which shows the effects random user separation in indoor scenarios

If the average random user separation increases in both LOS and NLOS and using Ricean fading channels, the sum-rate channel capacity become the same.

# Chapter 5

## Conclusion and Recommendation

### 5.1 Conclusion

Based on the simulation results obtained in chapter 4, the following conclusion has been given.

- In multi-user environment increasing the number of antenna elements at both transmitter and receiver side is increasing the channel capacity linearly. But, simply by increasing the number of antenna elements the channel capacity cannot be increased. Here, as it has been seen on the simulation results, antenna spacing and user separation plays the main role on the sum-rate channel capacities of (4xTX, 4xRX) MU-MIMO system in an indoor environment.
- In an indoor NLOS the antenna spacing from  $0.2\lambda$  to  $0.5\lambda$  is better to get optimum sum-rate channel capacity in indoor (4xTX, 4xRX) MU-MIMO BC . Hence, NLOS path is rich of scatterers, generally Rayleigh fading channels has been considered to calculate the sum-rate channel capacity.
- In an indoor LOS the antenna spacing greater or equal to  $0.5\lambda$  is better to obtain the optimum sum-rate channel capacity of (4xTX, 4xRX) indoor MU-MIMO BC . Since in LOS the channel is fixed, iid Gaussian non-fading channel is selected.
- Since indoor environment scenario consists of LOS and NLOS path Ricean fading channels is selected to calculate the sum-rate capacity of (4xTX, 8xRX) MU-MIMO BC channel capacity. Ricean fading channel is better than Rayleigh fading channel to obtain the optimum sum-rate channel capacity with the same antenna spacing at BS.
- In (4xTX, 4xRX) MIMO-MAC Sum-rate channel capacity, the effects of average separation distance of randomly distributed users in 25m coverage areas in

an indoor NLOS has been considered. In (4xTX, 4xRX) MIMO-MAC indoor NLOS, the average separation distance of randomly distributed users in 30m coverage areas should not be much closer to each other less than 4m to get finest sum-rate channel capacity. Since the channel is Rayleigh fading channel.

- In (4xTX, 4xRX) MIMO-MAC Sum-rate channel capacity, the effect of average separation distance of randomly distributed users in 10m coverage areas in an indoor LOS has been considered. In this scenario, generally the randomly distributed user should not be much closer to each other less than 2m since there is no scatterer. The channel is iid Gaussian non-fading channel.
- In (8xTX, 4xRX) MIMO-MAC Sum-rate channel capacity, the effects random user separation in indoor scenarios has been considered. In this case, since the fading channel is Ricean, the separation distance among randomly distributed user in both LOS and NLOS path has no much effects on the sum-rate channel capacity of MU-MIMO system.

## 5.2 Drawbacks

In this thesis work, the following drawback was observed. These are,

- In uplink (MIMO-MAC) of fading and non-fading channels, the correlated sum-rate channel capacity has no parameter of comparison. Which is in MIMO-MAC the correlated sum-rate channel capacity is equivalent to single user sum-rate channel capacity. Therefore, we compared the correlated sum-rate channel capacity to each other to get better user separation for optimum correlated sum-rate channel capacity.
- In this thesis work the correlated sum-rate channel capacity is limited to equal number of BS antennas and K-users with single antenna element on their device. Because, to obtain the Kronecker channel correlation model first we need to get antenna correlations. That is, to get correlated channel, we need to multiply both the transmitter and receiver antenna correlation with fading or non-fading channels.

## 5.3 Recommendation for Future Works

The following few promising future works were proposed.

- In this thesis work , it has been considered spatial correlation effects on the sum-rate channel capacity on different fading channels for indoor LOS and

NLOS where in both cases decisions are based on analytical-based channel correlation model. The use of physical channel model which is more accurate for indoor MU-MIMO sum-rate channel capacity could be interesting area to investigate.

- The results presented in this thesis work are based on the simulation results that the number of antennas at the BS and the number of k-users with single antenna element on their devices are assumed to be equal. And the channel state information is assumed to be known at both transmitter and receiver sides. The above two assumptions is not usually the case in real condition and studying the impact of real assumptions on indoor MU-MIMO sum-rate channel capacity evaluation need to be addressed.
- This thesis work is limited to antenna spacing effects on the sum-rate channel capacity of indoor MU-MIMO system which focuses only to obtain adequate antenna spacing but, because of the limited size of our equipment it is impossible increase the space between two adjacent antenna elements as we like. So, we have a limited equipment size. To overcome this problem to some extent, the idea of side-lobe canceller and beamformer should be investigated. These two ideas can handle the effects of the two adjacent antennas on each other. A study in this area is another work in multiuser environment.
- In this thesis work different correlation effects have been neglected. Using different correlation techniques e.g temporal correlation, phase correlation that can affect the indoor MU-MIMO sum-rate channel capacity. Therefore, spatial and temporal dynamics in indoor MU-MIMO is also another future research work.
- In this thesis work antenna correlation at base station and user separation at UE side considered without knowing antenna state. That is, excited and terminated antenna at both side should be considered to compute effects of antenna correlation in all ports on channel capacity. Therefore the idea of embedded element pattern in indoor MU-MIMO is also another future research work.
- This thesis work is limited to the effects of antenna correlation on channel capacity only without considering the order of diversity gain. Therefore effects of antenna mutual coupling will be another future research work in indoor MU-MIMO channel capacity.

# Bibliography

- [1] I. Poole *Multi-User MIMO*, <http://www.radio-electronics.com/info/antennas/mimo/multi-user-mu-mimo.php>. [Online] (November, 2014).
- [2] B. Z. Maha and R. Kosai *Multi User MIMO Communication: Basic Aspects, Benefits and Challenges*, Recent Trends in Multi-user MIMO Communications, December 4, 2013.
- [3] Professor R. W. Heath, *MIMO-communication*, <http://www.profheath.org/mimo-communication/multiple-user-mimo/>. [Online] (November, 2014).
- [4] H. Q. Ngo, *Performance Bounds for Very Large Multiuser MIMO Systems*, ISSN 0280-7971, November 12, 2012.
- [5] V. Stankovic, *Multi-user MIMO wireless communications*, November, 2006.
- [6] O. Edfors, F. Tufvesson and F. Rusek, *Indoor Multi User MIMO: Measured User Orthogonality and its impact on the choice of codings*, Lund University, Sweden, 2012.
- [7] T. Wu, Y.H. Kwon, Anthony C. K. Soong, R. W. Heath Jr., *Multiuser MIMO in Distributed Antenna Systems*, November, 2010.
- [8] M. Kyung and H. Mohaisen, *On Transmit Antenna Selection for Multiuser MIMO Systems with Dirty Paper Coding*, South Korea, September, 2009.
- [9] V. Jungnickel, T. Haustein, C. von Helmolt V. Pohl, *Antenna Spacing in MIMO Indoor Channels*, Berlin, Germany, 2002.
- [10] B. Holter, *On the capacity of the MIMO channel*, Norwegian University of Science and Technology, Department of Telecommunications, Norway, 2003.
- [11] J.W. Wallace, *Modeling the Indoor MIMO Wireless Channel*, IEEE Trans. on Antennas and Propagation, vol. 50, no. 5, pp. 591-599, May 2002.
- [12] J. Wallace and M. Jensen, *Statistical Characteristics of Measured MIMO Wireless Channel Data and Comparison to Conventional Models*, in Proc. IEEE Vehicular Technology Conference, vol. 2, no. 2, pp. 1078-1082, October 2001.

- [13] G. Caire and S. Shamai, *On the achievable throughput of a multi-antenna Gaussian broadcast channel*, IEEE Trans. on Inf. Theory., vol. 49, no. 7, pp. 1691-1706, July 2003.
- [14] M.H.M. Costa, *Writing on dirty paper*, IEEE Trans. on Inf.Theory, vol. 29, no. 12, pp. 439-441, May 1983.
- [15] N. Jindal, and A. J. Goldsmith S. Vishwanath, *On the capacity of multiple input multiple output broadcast channels*, in Proc. of the IEEE International Conference on Communications (ICC) , New York, April 2002.
- [16] B. Hochwald, and L. Swindlehurst C. Peel, *A vector-perturbation technique for near-capacity multi-antenna multi-user communication*, in Proc. of the 41st Allerton Conference on Communication, Control, and Computing October 2003.
- [17] R. F. H. Fischer, and J. B. Huber C.Windpassinger, *Lattice-reduction-aided broadcast precoding*, in Proc. 5th International ITG Conference on Source and Channel Coding (SCC), vol. 6, no. 2, pp. 403-408, January 2004.
- [18] D. Tse and P. Viswanath, *Fundamentals of Wireless Communication*, England, UK: Cambridge University Press, 2005.
- [19] Nimay Ch. Giri, *Capacity Performance Comparison of SISO and MIMO System for Next Generation Network (NGN)*, International Journal of Advanced Research in Computer Engineering Technology (IJARCET), vol. 3, no. 9, September 2014.
- [20] M. Herdin, H.A Ozcelik, and E. Bonek W. Weichselberger, *A Stochastic MIMO Channel Model with Joint Correlation of Both Link Ends*, IEEE Trans. on Wireless Comm.vol.5, no.1, January 16,2006.
- [21] L. Schumacher, K. Pedersen, P. Mogensen, and F. Frederiksen J. Kermoal, *A Stochastic MIMO Radio Channel Model with Experimental Validation*, IEEE J. Sel. Areas Comm., vol. 20, no. 6, pp. 1211-1226, August 2002.
- [22] G. Foschini, M. Gans, and J. Kahn D.-S. Shiu, *Fading Correlation and Its Effect on the Capacity of Multi-element Antenna Systems*, IEEE Trans. Comm., vol. 48, no. 3, pp. 502-513, March 2000.
- [23] F. Rashid-Farrokhi, J. Ling, and A. Lozano D. Chizhik, *Effect of Antenna Separation on the Capacity of BLAST in Correlated Channels*, IEEE Comm. Letters, vol. 4, no. 11, pp. 337-339, November 2000.

- [24] J. Kahn, and D. Tse C.-N. Chuah, *Capacity of Multi-Antenna Array Systems in Indoor Wireless Environment*, in Proc. IEEE Global Telecommunications Conf., vol. 4, pp. 1894-1899, 1998.
- [25] Tommi J., *HW Implementation of Indoor MIMO WLAN Channel Models*, IEEE 802.11-03/824r0, November, 2003.
- [26] Erceg V., *Indoor MIMO WLAN Channel Models*, IEEE 802.11 document 03/161r2, September, 2003.
- [27] C. A. Balanis, *Antenna Theory, Analysis and Design*, John Wiley Sons, Inc., New Jersey, 2005.
- [28] J. Lv, Y. Lu, Y. Wang, H. Zho and C.Y. Han, *Antenna Spacing Effect on Indoor MIMO Channel Capacity*, IEEE Conference Publishing, vol. 3, December, 2005.
- [29] S. Saunder, *Small cell Forum Release program*, <http://www.smallcellforum.org/about/what-we-do/20142015-round/>. [Online] (November, 2014)

# Appendix

## Appendix-A: MU-MIMO sum-rate channel capacity and MIMO MAC-BC duality

[2, 18]

For a MIMO system with  $N_T$  transmit and  $N_R$  receive antennas, we consider a K-user MIMO system over a flat fading MAC with  $M$  antennas at BS and single antenna at each UE. Denote  $H_K$  and  $X_K$  the channel matrix and the transmitted vector of K-UE . The received vector from user is

$$y = \sum_{k=1}^K H_K X_K + n \quad (5.1)$$

here  $n$  is a vector of complex additive white Gaussian noise (AWGN) samples with zero mean and unit variance.  $H_K$  are independent among different UEs and perfectly known at both the transmitter and the receiver. Therefore, the capacity of the channel is shown as,

$$C = \underset{Q_K}{\max} I(X; Y) \quad (5.2)$$

In which  $Q_K$  is the probability density function (PDF) of the transmit signal vector  $x$ , and  $I(X; Y)$  is the mutual information of random vectors  $x$  and  $y$ . Namely, the channel capacity is the maximum mutual information that can be achieved by varying the PDF of the transmit signal vector. From the fundamental principle of the information theory, the mutual information of the two continuous random vectors,  $x$  and  $y$ ; is given as

$$I(X; Y) = H(Y) - H(Y|X) \quad (5.3)$$

In which  $H(Y)$  is the differential entropy of  $y$  and  $H(Y|X)$  is the conditional differential entropy of  $y$  when  $x$  is given. Using the statistical independence of the two random vectors  $n$  and  $x$  in equation(5.1), we can show the following relationship:



$H(Y|X) = H(n)$  Then substituting into equation (5.3),

$$I(X; Y) = H(Y) - H(n) \quad (5.4)$$

Meanwhile, the auto-correlation matrix of  $y$  is given as,

$$\begin{aligned} R_{yy} &= E(yy^H) \\ &= E\left(\sum_{k=1}^K H_K X_K + n\right) \left(\sum_{k=1}^K H_K X_K + n\right)^H \\ &= \sum_{k=1}^K E(H_K X_K H_K^H X_K^H) + E n n^H \\ &= \sum_{k=1}^K E(H_K X_K X_K^H H_K^H) + N_O I_R \\ &= \sum_{k=1}^K H_K Q_K H_K^* + N_O I_R \\ &= N_O I_R + \sum_{k=1}^K H_K Q_K H_K^* \end{aligned} \quad (5.5)$$

$Q_K = E[X_K X_K^*] = \frac{P_t}{(\sigma_x^2)}$  is the transmitted signal energy. Then, the mutual information of  $y$  and  $n$  is respectively given as,

$$H(Y) = \log_2 \det(\pi e R_{yy}) \quad (5.6)$$

$$H(n) = \log_2 \det(\pi e N_o I_R) \quad (5.7)$$

Substituting into the following,

$$I(X; Y) = H(Y) - H(n)$$

$$I(X; Y) = \log_2 \det(\pi e R_{yy}) - \log_2 \det(\pi e N_o I_R) \quad (5.8)$$

Then, the channel capacity of MIMO MAC channel is expressed as

$$C_{MAC} = \left(\max_{tr(Q_K)}\right) I(X; Y) = \left(\max_{tr(Q_K)}\right) \log_2 \det\left(I_R + \sum_{k=1}^K H_K Q_K H_K^*\right) \quad (5.9)$$

Under individual power constraints MIMO MAC channel capacity can be modified

as,

$$C_{MAC} = \left( \max_{tr(\sum_{k=1}^K Q_K) \leq P_K} \right) I(X; Y) = \left( \max_{tr(Q_K) \leq P_K} \right) \log_2 \det \left( I_R + \sum_{k=1}^K H_K Q_K H_K^* \right) \quad (5.10)$$

Subjected to  $tr \left( \sum_{k=1}^K Q_K \right) \leq P_K, \forall_K$

Then based on duality principle of Gaussian MIMO MAC-BC with multiple transmit covariance constraints, we can obtain the MIMO BC sum-rate channel capacity. i.e. in Gaussian MIMO-BC associated optimization problem such as capacity computation and beamforming optimization are typically non-convex and cannot be solved directly. On feasible approach to this problem is to transform them into their dual MAC which is easier to deal with due to their convexity property. Based on this there are two types of BC-MAC duality. These are;

- Conventional BC-MAC duality
- Minimax BC-MAC duality

## Conventional duality

The conventional BC-MAC duality is established via BC-MAC signal transformation and has been successfully applied to solve beamforming optimization, SINR balancing, and capacity region computation. However, this conventional duality approach is applicable only to the case in which the BS of BC is subjected to single power constraints. Therefore;

- Under single sum power constraints the capacity region of BC is identical to that of dual MAC under the same power constraints.
- The channel matrix associated with dual MAC is the conjugate transposed channel matrix of BC, and the noise covariance matrixes of both channels are identity matrices.

## Minimax BC-MAC duality

The sum-rate maximization problem of a BC with multiple linear constraints has the solution as the dual MAC minimax optimization problem. Then the channel matrix of the dual MAC is the conjugate transposed channel matrix of the BC, and the noise covariance matrix of the dual MAC is unknown variable of the minimax optimization problem. Generally, based on the conventional duality principle the

dual BC sum-rate channel capacity under single sum power constraints become as follows:

$$C_{BC} = \left( \max_{tr(Q_K) \leq P} \right) I(X; Y) = \left( \max_{tr(Q_K) \leq P} \right) \log_2 \det \left( I_R + \sum_{k=1}^K H_K^* Q_K H_K \right) \quad (5.11)$$

Subjected to  $tr(Q_K) \leq P, \forall_K$

## Appendix-B: Simulation Algorithms

- **Step-1:** Input
  - Number of antennas at the BS
  - Number users
  - Carrier wavelength
  - Angular spread
  - Antenna spacing at BS and User separation
- **Step-2:** Using Jakes correlation model, calculate the transmitter and receiver antenna correlation coefficients independently i.e.

$$\rho(d) = \exp^{-j2\pi d/\lambda \cos\Phi} \quad (5.12)$$

- **Step-3:** Then calculate transmitter and receiver antenna correlation matrix separately.

$$R_{Tx}, R_{Rx} = \begin{bmatrix} 1 & \rho^* & \dots & \rho^{*(r-1)} \\ \rho & 1 & \dots & \rho^{*(r-2)} \\ \vdots & \vdots & \ddots & \vdots \\ \rho^{(r-1)} & \rho^{(r-2)} & \dots & 1 \end{bmatrix} \quad (5.13)$$

Where, r is number of transmitter or receiver antenna.

- **Step-4:** Use different stochastic models such as, iid Gaussian non-fading channel (Hz), Rayleigh channel (Hw) and Ricean channel (HR) depending on indoor scenarios i.e.

$$H_z = \text{randn}(n_R, n_T) + j\text{randn}(n_R, n_T) \quad (5.14)$$

$$H_w = \frac{1}{\sqrt{2}}(\text{randn}(n_R, n_T) + j\text{randn}(n_R, n_T)) \quad (5.15)$$

$$H_R = \sqrt{\frac{K}{(K+1)}}H_z + \sqrt{\frac{1}{(K+1)}}H_w \quad (5.16)$$

- **Step-5:** Using Kronecker channel modeling, calculate the correlated channel matrix between the transmitter and receivers antennas for step-4 indoor

scenarios i.e.

$$H = R_{Tx}^{\frac{1}{2}} H_z R_{Rx}^{\frac{1}{2}}$$

$$H = R_{Tx}^{12} H_w R_{Rx}^{\frac{1}{2}}$$

$$H = R_{Tx}^{\frac{1}{2}} H_R R_{Rx}^{12}$$

- **Step-6:** Use duality principles of MIMO MAC-BC.
- **Step-7:** Assume equal power allocation among BS antenna elements and based on individual power constraints at K-users.
- **Step-8:** Calculate correlated sum-rate channel capacity based on step 5 and 6 for both MAC and BC i.e.

$$C_{MAC} = \left( \max_{tr(\sum_{k=1}^K Q_K) \leq P_K} \right) \log_2 \det \left( I_M + \sum_{k=1}^K H_K Q_K H_K^* \right) \quad (5.17)$$

$$\text{Subject to } tr \left( \sum_{k=1}^K Q_K \right) \leq P_K, \forall_K$$

where  $P_K$  is individual power constraints,  $M$  is number BS antennas and  $Q_K = E[X_K X_K^*] = \frac{P_t}{(\sigma_t^2)}$ . And,

$$C_{BC} = \left( \max_{tr(\sum_{k=1}^K Q_K) \leq P} \right) \log_2 \det \left( I_R + \sum_{k=1}^K H_K^* Q_K H_K \right) \quad (5.18)$$

Subject to  $tr \left( \sum_{k=1}^K Q_K \right) \leq P, \forall_K$  Where  $P$  is the total transmitted power and  $N$  is number of users.

- **Step-9:** Compare with non-correlated sum-rate channel capacity.